University of Alberta

A CAPILLARY METHOD FOR LINE TENSION DETERMINATION

by

Ward Calvin Jensen ©

A thesis submitted to the Faculty of Graduate Studies and Research in partial fulfillment of the requirements for the degree of Master of Science

Department of Mechanical Engineering

Edmonton, Alberta
Fall 1997

National Library of Canada
Acquisitions and Bibliographic Services
395 Wellington Street
Ottawa ON K1A 0N4
Canada

Bibliothèque nationale du Canada
Acquisitions et services bibliographiques
395, rue Wellington
Ottawa ON K1A 0N4
Canada

Your file Votre référence

Our file Notre référence

The author has granted a non-exclusive licence allowing the National Library of Canada to reproduce, loan, distribute or sell copies of this thesis in microform, paper or electronic formats.

The author retains ownership of the copyright in this thesis. Neither the thesis nor substantial extracts from it may be printed or otherwise reproduced without the author's permission.

L'auteur a accordé une licence non exclusive permettant à la Bibliothèque nationale du Canada de reproduire, prêter, distribuer ou vendre des copies de cette thèse sous la forme de microfiche/film, de reproduction sur papier ou sur format électronique.

L'auteur conserve la propriété du droit d'auteur qui protège cette thèse. Ni la thèse ni des extraits substantiels de celle-ci ne doivent être imprimés ou autrement reproduits sans son autorisation.

0-612-22607-7

Canada

University of Alberta

Library Release Form

Name of Author: **Ward Calvin Jensen**

Title of Thesis: **A Capillary Method for Line Tension Determination**

Degree: **Master of Science**

Year this Degree Granted: **1997**

Permission is hereby granted to the University of Alberta Library to reproduce single copies of the thesis and to lend or sell such copies for private, scholarly, or scientific research purposes only.

The author reserves all other publication and other rights in association with the copyright in the thesis, and except as hereinbefore provided, neither the thesis nor any substantial portion thereof may be printed or otherwise reproduced in any material form whatever without the author's prior written permission.

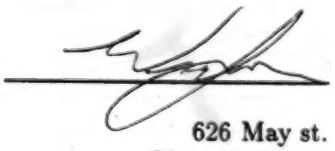

626 May st.
Elgin IL, 60120

October 3,1997

University of Alberta

Faculty of Graduate Studies and Research

The undersigned certify that they have read, and recommend to the Faculty of Graduate Studies and Research for acceptance, a thesis entitled "A Capillary Method for Line Tension Determination" submitted by Ward Calvin Jensen in partial fulfillment of the requirements for the degree of Master of Science.

Dr. D. Li

Dr. T. Forest

Dr. J. Elliott

October 3,1997

Abstract

Line tension is an important quantity in surface thermodynamics. A general Young Equation which applies to solid surfaces of revolution can be used with a conical capillary tube to determine line tension values. It is possible to determine the line tension by measuring the dependence of the contact angle, measured indirectly, on the curvature of a well prepared homogenous solid surface. Several conical capillary tubes were carefully prepared and tested with four members of the decane family: decane, dodecane, tetradecane, and hexadecane. The results of this experiment show a negative slope for the correlation of the cosine of the contact angle versus the curvature of the solid surface, supporting recent measurements indicating that line tension is positive. The results obtained for the magnitude of the line tension range from 4.5 to $6.9 \mu J m^{-1}$, further supporting recent work which would indicate that the line tension is of the order of $1 \mu J m^{-1}$.

Acknowledgement

This work was supported by the Natural Sciences and Engineering Research Council of Canada. Without their support I would not have been able to return to the University to pursue an advanced engineering degree. I would also wish to thank Dr. Dongqing Li for his support, understanding and help in completing this work.

Contents

1 Introduction **1**
- 1.1 Previous work 6
- 1.2 Theory for inclined surfaces 9
- 1.3 Measurement requirements 11
- 1.4 Curve fitting 13

2 Design Considerations **15**
- 2.1 Liquids and surface coatings 15
- 2.2 Tube design 17
- 2.3 Measurement apparatus 21
- 2.4 Calibration 25
- 2.5 System accuracy 26

3 Results and Discussion **28**
- 3.1 Initial test results 28
- 3.2 Re-polished tubes 31

4 Conclusions **37**

A Tabular data **39**

B Sample Calculations **44**

C Statistical analysis **50**

D Dodecane Statistical Calculations **52**

E Grinding and polishing **54**

Bibliography **55**

List of Tables

3.1 Calculated results from $\cos\theta$ vs $\cos\beta/R$ 34
3.2 Comparitive results from ADSA and ACRPAC techniques 34

A.1 Properties used in calculations 39
A.2 Decane measured data and calculated intermediate results 40
A.3 Dodecane measured data and calculated intermediate results 41
A.4 Tetradecane measured data and calculated intermediate results 42
A.5 Hexadecane measured data and calculated intermediate results 43

B.1 Values used in calculations 46

List of Figures

1.1 Sessile drop shown from above and from the side . . . 3
1.2 Conical capillary tube 12

2.1 Drawn tube with capillary rise of water 19
2.2 Sketch of conical capillary tube in glass rod 20
2.3 Measurement equipment 22
2.4 Measurement apparatus 22
2.5 Modified tube clamp 23
2.6 Cross section of tube in reservoir 24

3.1 Possible errors in assumption of $\cos\theta_\infty$ 29
3.2 Results from original polishing 30
3.3 Results from decane 32
3.4 Results from dodecane 32
3.5 Results from tetradecane 33
3.6 Results from hexadecane 33

List of Symbols

A	Liquid vapor interface area
B	Bulk phase
H	Height of capillary rise
J	Mean curvatue
L	Length of three-phase contact
N	Number of Moles
P	Pressure
R	Three-phase contact radius
S	Entropy
T	Temperature
U	Internal Engergy
V	Volume
X	Horizontal axis displacement
Y	Vertical axis dispacement
b	Minimum capillary tube diameter
g	Gravity
x	Horizontal Axis Displacement
y	Vertical Axis Displacement
θ	Contact angle
θ_∞	Contact angle for infinite drop
θ_a	Advancing contact angle

θ_r	Receding contact angle
β	Capillary tube wall angle
γ	Suface Tension
σ	Line Tension
μ	Chemical Potential
Ψ	Grand Canonical Potential
ρ	Density
ΔP	Pressure Gradient

Subscripts

l	Liguid
s	Solid
v	Vapor
sv	Solid-Vapor
sl	Solid-Liquid
lv	Liquid-Vapor

Chapter 1

Introduction

Line tension is a quantity with specific applications in surface thermodynamics. Line tension has been studied with disagreements as to the value in both magnitude and sign. Li and Lin [2] have proposed that a simple apparatus could be fabricated enabling one to easily determine line tension from a single capillary measurement. This study focuses on using such an apparatus and methodology to determine, with confidence, line tension for several liquids.

Gibbs' seminal work[3] - [5] in classical and surface thermodynamics is the basis for this work and is briefly outlined below as it applies to this study. For a simple thermodynamic system consisting of a single and homogenous bulk phase there exists a fundamental relation which relates the internal energy, U, of the system to the extensive parameters; entropy S, volume V and the mole numbers $N_1, ..., N_r$ for r chemical components ie.

$$U = U(S, V, N_1, ..., N_r) \tag{1.1}$$

The extensive parameters are those that are directly related to the size of the system. We are often interested in the changes in the internal energy with respect to the change in the extensive properties. The first differential for the change in the internal energy of the system dU can be shown as:

$$dU = (\frac{\partial U}{\partial S})_{V,N_1,...N_r} dS + (\frac{\partial U}{\partial V})_{S,N_1,...N_r} dV + \sum_{i=1}^{r} (\frac{\partial U}{\partial N_i})_{S,V,...N_r} dN_i \tag{1.2}$$

The partial derivatives appearing in Equation 1.2 are called intensive parameters and are independent of the size of the system. The conventional notation used is:

$$\begin{aligned}(\frac{\partial U}{\partial S})_{V,N_1,...N_r} &\equiv T \\ -(\frac{\partial U}{\partial V})_{S,N_1,...N_r} &\equiv P \\ (\frac{\partial U}{\partial N_j})_{S,V,...N_r} &\equiv \mu_j \end{aligned} \tag{1.3}$$

where T is the bulk temperature, P is the pressure and μ_j is the chemical potential of the jth component expressed in energy per mole N. With this notation Equation 1.2 becomes

$$dU = TdS - PdV + \mu_1 dN_1 + ... + \mu_r dN_r \tag{1.4}$$

For more complex systems consisting of several bulk phases the internal energy can be expressed as a sum of the energies for each bulk phase. For a system which consists of two bulk phases arbitrarily referred to as α and β, the internal energy could then be written as

$$U = U^\alpha + U^\beta \tag{1.5}$$

where $U^\alpha$and U^β represent the energy in the α phase and β phase respectively. For systems with phases in contact there is an interface between the phases which adds to the total internal energy for the system. The interface or boundary is only significant in small systems where the free energy of the boundary is comparable to the bulk energies. The interface or surface quantities, called excess quantities are the differences between the total system quantities and the sum of the bulk phase quantities. If we consider two phases, α and β in contact then the excess energy or surface energy, U^A, distributed over the interface area can be expressed as

$$U^A = U - U^\alpha - U^\beta \tag{1.6}$$

The energy U^A can also be expressed as a function of extensive parameters.

$$U^A = U^A(S^A, A, N_1^A ... N_r^A) \tag{1.7}$$

The differential expression

$$dU^A = TdS^A + \gamma dA + \sum_{i=1}^{r} \mu_i dN_i^A \tag{1.8}$$

introduces the term γ which is defined as;

$$(\frac{\partial U^A}{\partial A}) \equiv \gamma \tag{1.9}$$

The surface tension, γ, is distributed over the area A of the two phase interface. Surface tension is the free energy per unit area or the force that minimizes the area of a two phase interface.

For systems with at least 3 bulk phases there can be, in addition to an area of contact, a line of contact. Figure 1.1 shows a liquid drop resting on a solid surface in a vapor environment. This system consists of three bulk phases; the solid bulk phase, the liquid bulk phase and the saturated liquid-vapor bulk phase.

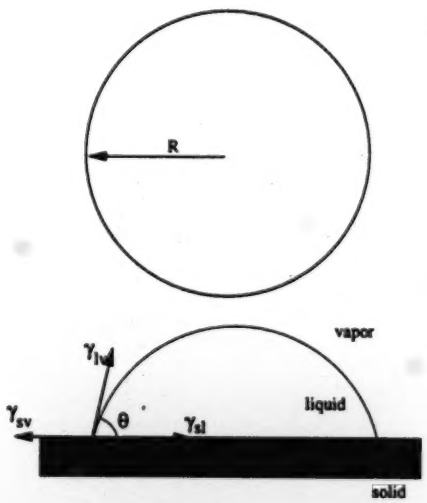

Figure 1.1: Sessile drop shown from above and from the side

Many are familiar with the concept of surface tension, eg liquid-vapor surface tension, which in this case is distributed over the area of the partial hemisphere. This same drop viewed from above, forms a circle in the plane of the solid. This circle represents the solid-liquid-vapor interphase and has a tensile force acting through it, which if assumed to be positive, would tend to minimize its perimeter or length and increase the contact angle, θ, shown. This tensile force is the line tension that is to be measured.

Line tension, σ, is a quantity that appears in surface thermodynamics and can be described in analogy to surface tension, γ [1].

$$(\frac{\partial U^l}{\partial L}) \equiv \sigma \tag{1.10}$$

The equilibrium conditions can be derived from minimizing the energy of the system. A widely used formalism which greatly simplifies this analysis is know as the "grand canonical" formalism. The grand canonical potential, often represented as Ψ[26], is a simple substitution of other extensive parameters in place of the energy U. This formalism is applicable in systems where conditions are such that the temperature and chemical potential remain constant in all phases. The grand canonical potentials for an area of interphase, Ψ_A, a three phase line interface, Ψ_L, and a bulk phase, Ψ_B, are written as

$$\begin{aligned}
\Psi_A &= U^A - TS^A - \sum_{i=1}^{r} \mu_i dN_i^A = \gamma A \\
\Psi_L &= U^L - TS^L - \sum_{i=1}^{r} \mu_i dN_i^L = \sigma L \\
\Psi_B &= U^B - TS^B - \sum_{i=1}^{r} \mu_i dN_i^B = -PV
\end{aligned} \tag{1.11}$$

The total grand canonical potential for a system such as that shown in Figure 1.1 where the drop is assumed to be moderately curved and free from any magnetic or electric fields is

$$\Psi_{total} = \Psi_l + \Psi_v + \Psi_{lv} + \Psi_{sv} + \Psi_{sl} + \Psi_L \tag{1.12}$$

where the subscripts l,v stand for the liquid and vapor phase respectively. The subscripts lv,sv,sl stand for the liquid-vapor, solid-vapor and solid-liquid interface respectively and L stands for the three phase linear interphase.

If we consider the solid, liguid, vapor system, the total free energy Ψ_{total} is a minimum at equilibrium. This implies that

$$d\Psi_{total} = -P_l dV_l - P_v dV_v - P_s dV_s + \gamma_{lv} dA_{lv} + \gamma_{sv} dA_{sv} + \gamma_{sl} dA_{sl} + \sigma dL = 0 \tag{1.13}$$

The constraints for the system are that the total volume, $V_l + V_v$, is constant as is the area $A_{sv} + A_{sl}$ and the solid volume V_s remains

constant. This implies that $dV_l = -dV_v$ and $dV_s = 0$ $dA_{sl} = -dA_{sv}$. Substituting into Equation 1.13

$$d\Psi_{total} = (P_v - P_l)dV_l + (\gamma_{sl} - \gamma_{sv})dA_{sl} + \gamma_{lv}dA_{lv} + \sigma dL = 0 \quad (1.14)$$

Re-arranging and manipulating Equation 1.14

$$d\Psi_{total} = \left[-(P_l - P_v) + \gamma_{lv}(\frac{\partial A_{lv}}{\partial V_l})\right] dV_l +$$

$$\left[\gamma_{lv}(\frac{\partial A_{lv}}{\partial A_{sl}}) - (\gamma_{sv} - \gamma_{sl}) + \sigma(\frac{\partial L}{\partial A_{sl}})\right] dA_{sl} = 0 \quad (1.15)$$

Since the variations dA_{sl} and dV_l are arbitrary, it is necessary and sufficient that the factors of these variations are zero. This produces a form of the Laplace Equation

$$P_l - P_v = \gamma_{lv}(\frac{\partial A_{lv}}{\partial V_l}) \quad (1.16)$$

and the Young's Equation.

$$\gamma_{lv}(\frac{\partial A_{lv}}{\partial A_{sl}}) + \sigma(\frac{\partial L}{\partial A_{sl}}) = \gamma_{sv} - \gamma_{sl} \quad (1.17)$$

in general

$$\frac{\partial A_{lv}}{\partial V_l} = \frac{1}{R_1} + \frac{1}{R_2} = J \quad (1.18)$$

where J is the mean curvature. For a spherical section used in the analysis of a sessile drop $J = 2/R$, where R is the spherical radius. For a spherical section

$$\begin{aligned} \frac{\partial A_{lv}}{\partial A_{sl}} &= \cos(\theta) \\ \frac{\partial L}{\partial A_{sl}} &= \frac{1}{R} \end{aligned} \quad (1.19)$$

substituting Equation 1.19 into Equations 1.16 and 1.17 produces two common equations in surface thermodynamics. The Laplace Equation

$$P_l - P_v = \gamma_{lv}\frac{2}{R} \quad (1.20)$$

and the modified Young's Equation

$$\gamma_{lv}\cos\theta = (\gamma_{sv} - \gamma_{sl}) - \frac{\sigma}{R} \quad (1.21)$$

Note that for large drops, $R \to \infty$, the modified Young Equation reduces to the classical Young's Equation

$$\cos\theta_\infty = \frac{\gamma_{sv} - \gamma_{sl}}{\gamma_{lv}} \tag{1.22}$$

The linear relationship between $\cos\theta$ and $1/R$ can be seen clearly when Equation 1.22 is combined with Equation 1.21 to produce

$$\cos\theta = \cos\theta_\infty - \left(\frac{\sigma}{\gamma_{lv}}\right)\left(\frac{1}{R}\right) \tag{1.23}$$

1.1 Previous work

Several studies [6]-[9] have been done using sessile drops to evaluate the line tension, σ, through a drop size dependance on contact angle θ. The modified Young Equation, Eq. 1.23, which was developed above and in more detail in the generalized theory of capillarity [38], predicts a linear relationship between $\cos\theta$ and $1/R$, the inverse of the contact radius. The slope of the line from this linear relationship is $-\sigma/\gamma_{lv}$ assuming that line tension, σ, and liquid-vapor surface tension, γ_{lv}, are constant. Since γ_{lv} is always positive, Eq. 1.21 also predicts that as the contact radius increases, the contact angle, θ, decreases for positive line tension. Theoretical studies designed to determine line tension generally use the modified Young Equation. It is significant that there is no consensus as to the magnitude of line tension or even as to the sign. Gibbs [27] had speculated in a footnote without further proof that "..linear tension there mentioned may have a negative value" De Feijter and Vrij [29] predict that line tension may be positive or negative depending on the system. Rowlinson and Widom [30] also concluded that line tension can be of either sign based on their three-phase model.

Experimental studies using the dependency of contact angle on the drop size, or radius of the three-phase contact line, do not agree on the sign of line tension. Ponter and Boyes [16, 17] showed through their tests that there are opposite trends in the above dependency. This would indicate that line tension can assume either sign. Ponter and Yekta-Fard [18, 19] also showed both trends depending on the environment. Still others conclude from their studies that a dependency does not exist between contact angle and drop size.

Steigmann and Li [24, 25] have shown that for a thermodynamically stable equilibrium, a positive line tension is required.

The size or magnitude of the values obtained through experiments is also inconsistent. Drelich and Miller [20]-[22] found a range of six orders of magnitude as their results would indicate values from $-10^{-6}\mu Jm^{-1} to -1\mu Jm^{-1}$. Good and Koo [6] found similar results. Ponter and Boyes [16, 17] and Ponter and Yekta-Fard [18, 19] found positive values in the range of $1 - 10\mu Jm^{-1}$. Harkins [28] and Buff and Saltsburg [29] estimated from their theoretical models that line tension is of the order of $10^{-11} - 10^{-10}N$ for a non-volatile oil lens on water. For similar a system of an oil lens on water Harkin [28] reports values of $2.0 * 10^{-5}\mu Jm^{-1}$, while Langmuir [23] reports values of approximately $60\mu Jm^{-1}$. Gaydos and Neumann [7], Li and Neumann [8] and Duncan et al. [9] report a contact angle dependency on drop size indicating that line tension is positive and of the order of $1\mu Jm^{-1}$ when using high quality surfaces.

It does not seem possible that line tension could assume both positive and negative values. For systems that are thermodynamically similar, one would expect a consistent sign and magnitude. The range that covers several orders of magnitude should also be of concern. Generally line tension experiments are developed measuring contact angle dependance on drop size with the results applied to the modified Young Equation, Eq. 1.21. This equation assumes that the surface is ideal. It should be perfectly smooth, homogenous and free from any surface defects. The preparation of a perfect surface is of course impossible and a preparation of a suitable surface is extremely difficult. Li [1] explains that extremely minor surface imperfections including defects, roughness or surfaces that are heterogenous can lead to misleading interpretation of contact angle data. The models Li used to simulate heterogenous surfaces or patches and surface imperfections can explain the positive and negative dependance of contact angle on drop size and the data that shows no correlation.

The angle, θ, in the modified Young Equation is the equilibrium contact angle. Generally, for a surface that is not carefully prepared, there exists a range of angles that give rise to a stable equilibrium. For a non-ideal surface the range may be as large as $50 - 90°$ with the larger, advancing contact angle θ_a, developing as the drop grows and advances across the surface and the smaller angle, termed the

receding angle, θ_r, which develops as the drop recedes across the surface. This difference between θ_a and θ_r is the well noted [10]-[15] contact angle hysteresis. In developing larger drops, vibrations can be induced that cause the three phase line to move and result in the receding contact angle to be measured. The advancing contact angle, θ_a, on a carefully prepared surface is the desired angle to use[11] in the modified Young Equation , Eq.1.21. Additionally the drops must be grown carefully to minimize induced vibrations in the system.

The measurement of the contact angle needs to be as precise as possible since there is usually a very limited range of angles, typically 5 degrees, measured for the typical range in drop size of a few millimeters. A goniometer, which is often used for measuring contact angles, can produce misleading results if not carefully used, since it is difficult to produce highly repeatable readings with this instrument which is sensitive to operator subjectivity. Accuracy of $\pm 2°$ in contact angle is typical [33].

The Axisymmetric Drop Shape Analysis (ADSA)[35]-[37] has been used in a drop size dependance of contact angle experiment with consistent and repeatable results that are essentially free of the subjective measurements of an operator. A brief over-view is given here.

The shape of a drop is governed by the Laplace Equation, Eq. 1.31. The camera used with the ADSA program digitizes the drop and analyses the image. The drop profile is determined from the density gradients between contiguous pixels. A calibration grid corrects for distortion and scaling factors. The Laplace Equation is parameterized and three first order differential equations are solved simultaneously. With the drop profile and the density of the liquid the program calculates the liquid-vapor surface tension, the contact angle, surface area, drop volume and the radius of the three phase contact circle. The surfaces are carefully prepared and coated [9, 1] with fluorochemical coating FC-721, a 3M $Fluorad^{TM}$ product that produces a durable surface with low values of surface energy. Using the ADSA method and equipment Li [9, 1] has shown line tension to be positive with an order of magnitude of $1 \mu J m^{-1}$ for several liquids.

1.2 Theory for inclined surfaces

The modified Young Equation is applicable only to a horizontal surface. If the surface is inclined, this equation does not describe the equilibrium conditions. In modeling multi-phase systems, it is often necessary to consider inclined surfaces or surfaces of revolution. For example; bubble nucleation will take place preferentially at defects in solid surfaces which can be modeled as conical crevices [31]. It has been shown that the three-phase region which is partially controlled or influenced by line tension has a significant role in the rate of growth of nucleating bubbles and the heat transfer rate [32]. Capillary condensation in a porous medium may also be modeled in a conical crevice since the curvature of the three phase line may vary continuously.

The model used for the system with an inclined surface is shown in Figure 1.2. A full derivation of the mechanical equilibrium condition can be found in other sources [2]. A derivation is outlined below and follows an analysis similar to that of a sessile drop. The equilibrium conditions can be found by minimizing the grand canonical potential, Ψ_{total}, with the intensive parameters being held constant.

$$\begin{aligned} d\Psi_{total} &= -P_l dV_l - P_v dV_v - P_s dV_s + \gamma_{lv} dA_{lv} \\ &+ \gamma_{sv} dA_{sv} + \gamma_{sl} dA_{sl} + \sigma dL = 0 \end{aligned} \tag{1.24}$$

The constraints are that the total of the bulk volumes is constant as is the the total of the surface area for the solid-vapor and solid-liquid interface, and $dV_s = 0$ This leads to:

$$d\Psi_{total} = (P_v - P_l)dV_l + (\gamma_{sl} - \gamma_{sv})dA_{sl} + \gamma_{lv} dA_{lv} + \sigma dL = 0 \tag{1.25}$$

which is the same as Equation 1.14 from the analysis of a sessile drop. With the assumption that the volume of the liquid drop remains constant, ie V_l = constant, and $dV_l = 0$, we arrive again at the Young's Equation.

$$\gamma_{lv}(\frac{\partial A_{lv}}{\partial A_{sl}}) + \sigma(\frac{\partial L}{\partial A_{sl}}) = \gamma_{sv} - \gamma_{sl} \tag{1.26}$$

From the geometry for a conical surface the following geometrical relationships can be derived

$$\frac{\partial L}{\partial A_{sl}} = \frac{\cos\beta}{R}\ ; \qquad \frac{\partial A_{lv}}{\partial A_{sl}} = \cos\theta \tag{1.27}$$

Substituting Equation 1.27 into Equation 1.26 results in the General Young Equation,

$$\cos\,\theta = \cos\,\theta_{\infty} - \frac{\sigma\cos\beta}{\gamma_{lv}R} \tag{1.28}$$

which is the equilibrium condition for a sessile drop in a conical crevice where the drop has moderate curvature. Moderate curvature is found in systems where the sessile drop radius, R, is less than 4 or $5mm$. The other significant assumption is that the solid surface is ideal and the local geometry describes a perfect conical surface. With these assumptions the three-phase contact line will be described by a circle of radius R. For systems where the geometry is such that the radius is not constant at a given horizontal plane, then the radius R is replaced by ρ, the local radius of curvature.

$$\cos\,\theta = \cos\,\theta_{\infty} - \frac{\sigma\cos\beta}{\gamma_{lv}\rho} \tag{1.29}$$

The correlation between the angle of inclination of the solid, the contact angle and line tension has been derived. It has been suggested to use this mechanical equilibrium condition, the General Young Equation Eq. 1.28 in an alternate strategy to determine line tension. Li and Lin [2] concluded that line tension could be determined from a single capillary height measurement. The remaining necessary parameters could be found in published literature or determined from the geometry of the tube. The tube angle from horizontal, β, is assumed to be constant over the length of the tube and can be measured after manufacturing. The three-phase radius R is a linear function of the the capillary rise H. ie

$$R = \frac{H}{\tan\beta} + b \tag{1.30}$$

The liquid-vapor surface tension, γ_{lv} and the contact angle for a theoretically infinite drop, θ_{∞}, can be either measured independently or found in published literature. The main advantage of this method is that the contact angle, θ, does not have to be measured directly, but can be determined from geometrical and surface properties. This

would eliminate a major source of error in conventional sessile drop experiments without the significant investment required using the ADSA method. The contact angle, θ, can be derived as follows: The Laplace Equation

$$\Delta P = \frac{2\gamma_{lv}}{r} \tag{1.31}$$

is substituted into an equation used to calculate pressure difference based on capillary height, H ie.

$$\Delta P = \Delta \rho g H \tag{1.32}$$

when Eq. 1.32 is substituted into Eq. 1.31, this results in

$$\Delta \rho g H = \frac{2\gamma_{lv}}{r} \tag{1.33}$$

$$r = \frac{2\gamma_{lv}}{\Delta \rho g H} \tag{1.34}$$

The contact angle, θ, can be determined from the tube geometry and the local radius of the capillary tube at the height H;

$$R = r \sin(\beta - \theta) \tag{1.35}$$

substituting Eq. 1.34 into Eq. 1.35 and solving for θ results in

$$\theta = \beta - \sin^{-1}\left(\frac{\Delta \rho g H R}{2\gamma_{lv}}\right) \tag{1.36}$$

Theoretically, Eq. 1.28 and Eq. 1.36 can be solved for line tension using published or previously measured parameters and those described above that can be derived from the capillary rise, H. Given this input, line tension, σ can be evaluated. It is known that accuracy in obtaining a capillary rise of the order of a micrometer is obtainable using a cathetometer [33]. It was speculated that using this method, line tension could be determined repeatably using a single measurement of capillary height to an accuracy of at least the same order of magnitude as the line tension itself.

1.3 Measurement requirements

To complete the analysis described using a conical capillary tube as shown in Figure 1.2 it is necessary to measure β before the

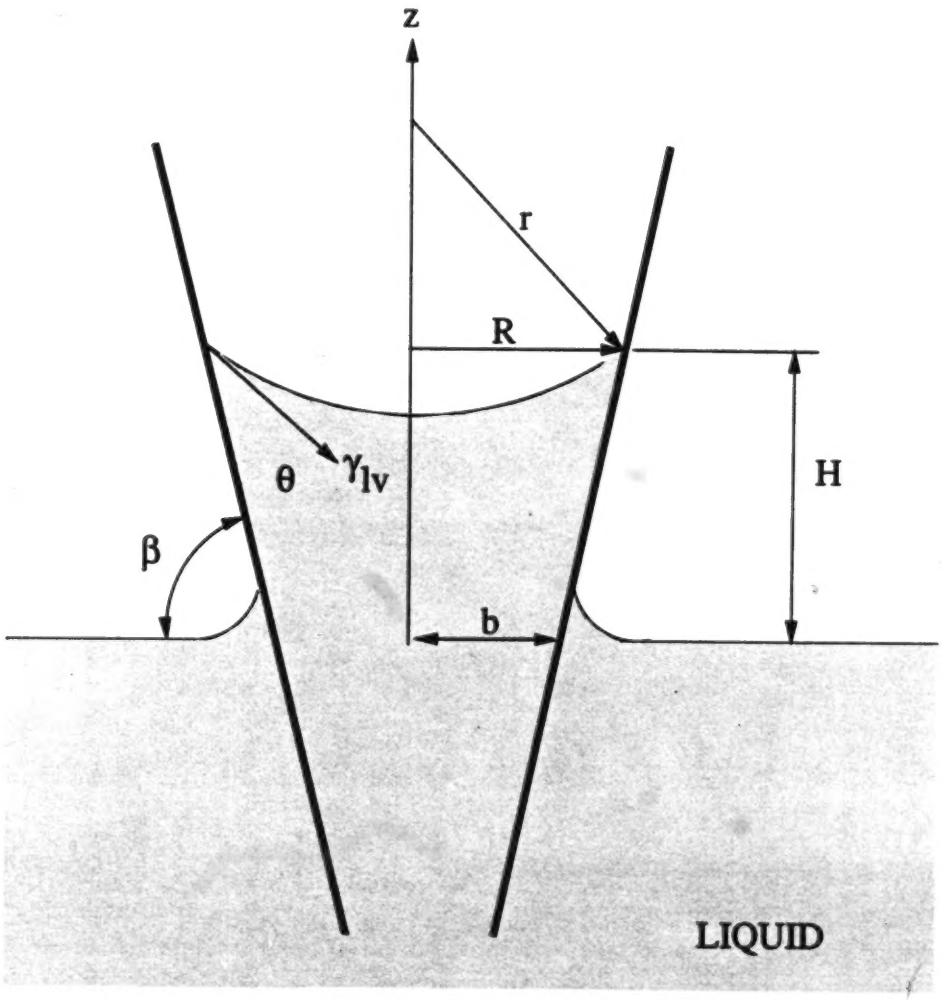

Figure 1.2: Conical capillary tube

experiment and determine the linear function in Eq. 1.30. The manufacturing of a suitable tube would seem to be simple as would the determination of the capillary rise H.

The measurement of b in Eq. 1.30 presents difficulties. The dimension b is the inside radius of the tube at a position of equal height with the free surface. It does not seem possible that b can be predetermined as can the tube angle β. Even if the region were accurately marked prior to the experiment, it would be difficult to establish that it was at the free surface since that region is obscured by a meniscus that forms around the tube rising from the free surface. In addition, if the tube was subsequently lowered or raised the value of b would change. If the bottom or top of the tube were measured and used to calculate either the radius, R, or free surface radius, b, an addition height measurement would be required in that relationship. It would appear that two geometrical measurements are needed to complete the evaluation of the mechanical equilibrium.

The most obvious choice of parameters to measure would be the capillary height, H, and the diameter of the meniscus which is simply twice the value of the three-phase radius, R. The contact angle could then be calculated directly from Equation 1.36. The line tension could then be calculated by re-arranging Equation 1.29

$$\sigma = \gamma_{lv} R \frac{(\cos\theta_\infty - \cos\theta)}{\cos\beta} \tag{1.37}$$

and substituting Equation 1.36

$$\sigma = \gamma_{lv} R \frac{\cos\theta_\infty - \cos\left[\beta - \sin^{-1}\left(\frac{\Delta\rho g H R}{2\gamma_{lv}}\right)\right]}{\cos\beta} \tag{1.38}$$

Line tension could thus be determined directly with two measurements of R and H on the capillary system. The remaining parameters could be measured before or obtained from other experiments or published literature.

1.4 Curve fitting

Most previous methods, such as those described in Section 1.1, to determine line tension used sessile drops to evaluate the line tension, σ, through a drop size dependance on contact angle θ. Drop size, or

more specifically, $1/R$, is plotted against the cosine of the contact angle, θ. From the slope of this relationship, $-\sigma/\gamma_{lv}$, line tension is determined. Several test are performed and a correlation coefficient is calculated. In addition, the linear relationship is used to extrapolate a value of $\cos\theta_\infty$. This is the theoretical value of $\cos\theta$ for an infinite drop where $1/R \to 0$.

Measuring line tension with conical capillary tubes as described in the previous section uses previously measured, or extrapolated, values of $\cos\theta_\infty$ as seen in Equation 1.38. This input can be eliminated if line tension is determined using curve fitting. From the general Young's Equation, eq 1.28, it can be seen that slope of the relationship for $\cos\theta$ vs. $\cos\beta/R$ is $-\sigma/\gamma_{lv}$. From this, line tension can be calculated if multiple measurements are taken. It eliminates a possible source of error in $\cos\theta_\infty$. The values for the correlation coefficients can be compared to similar analysis using sessile drops. The primary advantage of using conical capillary tubes is retained; the contact angle, θ, does not need to be measured. Since θ_∞ does not have to be used from previous values and included in the calculation of line tension, a source of uncertainty is then removed from the calculations.

Chapter 2

Design Considerations

2.1 Liquids and surface coatings

It was decided to test several liquids to evaluate line tension. The chemicals originally selected were;decane, dodecane, methyl salicylate, ethylene glycol and glycerol. These were selected to provide a direct comparison to the results of Li [9]. Initial tests of measurability failed for methyl salicylate, ethylene glycol and glycerol. These did not produce a capillary rise above the meniscus formed on the outside of the tube and hence the needed capillary height and three-phase diameter was obscured and hence un-measureable. Four saturated unbranched acyclic hydrocarbons were then chosen; decane, dodecane, tetradecane and hexane. It was expected that the decane family would have similar values for line tension since the surface tension values are similar. Physical properties and surface properties using the ADSA technique were available for these chemicals [1, 34] including values of line tension to use as a comparison. It should be noted that all tests conducted at a constant temperature of $20°C$ and hence published values of liquid density could be used.

The tests done with these members of the decane family by Li et. al. were done with sessile drops on carefully prepared surfaces [1]. The surface of contact must not only be a smooth surface, but it must also be homogenous and not react with or dissolve in the chemicals that it is tested with. The surface must have a low surface energy such that it repels the chemical tested and forms a finite and measurable contact angle. An uncoated surface such as glass has a

high surface energy. For a surface with a high surface energy the solid-vapor surface tension, γ_{sv} will be much larger than the solid-liquid surface tension, γ_{sl}. From Figure 1.1 it can be seen that the effect will be to "flatten" the drop by pulling the edges outward and reducing the contact angle. This is also referred to as wetting. If we consider Equation 1.21 and ignore for the moment the effect of line tension and re-arrange, we get

$$\cos\theta = \frac{\gamma_{sv} - \gamma_{sl}}{\gamma_{lv}} \tag{2.1}$$

Generally as γ_{sv} increases , the contact angle θ decreases. Wetting surfaces, ie those with high surface energy, have large capillary rises and contact angles that are small and difficult to measure.

Coatings are used for two purposes. Primarily, they are used to produce a surface that is hydrophobic, ie has a low surface energy and produces larger contact angles. Secondarily the coating helps provide a smooth homogenous surface by covering and filling small voids and surface defects. The coatings considered for this application were FC721 FC722 and FC725. These are 3M brand anti-migration coatings that are predominantly used in industry to repel liquids having low surface tension. They are used as barriers that prevent lubricant migration from critical wear zones such as found in bearings. Other uses include protective coating for electrical components. FC722 was selected for use because it had the lowest reported surface energy and it provided a good comparison to contact angle measurements previously performed with FC721 [1]. FC722 is the replacement for FC721 which has been discontinued. FC722 contains the same fluorochemical polymer but is dissolved in a solvent blend that does not harm the ozone layer as could the Freon base of FC721. FC722 has similar properties to FC721 including surface energy.

It was essential that the coatings be applied in a controlled manner so that the surfaces created were smooth and free of defects. Previous work measuring contact angles on glass plates required that the plates be dipped and that the retraction be rigorously controlled. The application to tubes requires that the drainage from the tube be controlled. The coating, was controlled by controlling the rate of drainage of FC722 from the tube.

Three or four of the capillary tubes that were created could be coated at once in a very simple apparatus. The cleaned tubes were

placed on top of each other in a syringe with sufficient diameter to accommodate them. The syringe was then filled with FC722 and drainage was controlled by restricting the flexible tubing attached to the syringe outlet, so that liquid level passed each tube slowly and evenly. With this method the FC722 could be easily collected for re-use.

Several measurements could be made from one tube before it had to be cleaned. To clean the tubes they were first rinsed with acetone to remove any particles. The tubes and any other glass used were then placed in a beaker of diluted nitric acid and placed in an ultra-sonic cleaner for 10-20 minutes before they were removed and rinsed. The process was repeated to ensure that the tubes were clean. The tubes were re-coated with FC722 and allowed to dry at least 12 hours.

2.2 Tube design

It can be seen from Equation 2.2

$$H = \frac{2\gamma_{lv}}{\Delta\rho g R}\sin(\beta - \theta) \tag{2.2}$$

which is derived from Equation 1.36 that the capillary rise H is inversely proportional to the tube radius, R. A tube made with a sufficiently small diameter, would therefore produce a significant capillary rise. A large rise should be easier to measure, and the relative error of $\epsilon H/H$, where H is the capillary rise or height and ϵH is the error in height, would be minimized.

The first tubes created for initial evaluation were made from glass tubing with an internal diameter of approximately 1mm. These tubes were heated over an open flame and pulled or drawn to near fiber thickness in the middle heated region. It was thought that from such a tube it should be possible to find a region where the diameter changed linearly over a given length. Initial tests of these tubes did produce such regions and significant capillary rises, but of concern for these tubes was the sensitivity of the calculated line tension to the uncertainty in the wall angle β. This sensitivity can be expressed by Equation 2.3

$$\frac{\partial\sigma}{\partial\beta} = \sec\beta[(\cos\theta_\infty - \cos\theta)\tan\beta - \sin\theta]R\gamma_{lv} \tag{2.3}$$

From Equation 2.3 it can be seen that as β approaches 90 degrees, or the conical tube becomes cylindrical, the uncertainty in line tension approaches infinity, since $\sec\beta \rightarrow \infty$. The tubes that were created from heated and drawn tubing had tapers but the wall angles were very nearly 90 degrees over most of the tapered length. For the very small diameter tubes it became apparent that the uncertainty in line tension was often much greater than the line tension itself. Such small diameter tubes also introduced a drainage problem for the surface coatings that had to be applied. The coating liquid could not drain from most of these small tubes or drained in such a fashion as to created blockage in the tube as bubbles of coating formed and dried.

Larger tubing was used to overcome drainage problems and introduce smaller β angles. Several such tubes were created and coated. These were initially tested on water to establish a method for measuring the three-phase contact diameter. Figure 2.1 shows the meniscus formed with water in the tube. When the tubes were examined with liquid in them, an accurate reading of the diameter could not be obtained. The nature of the tube itself created reflection and refraction patterns near the wall that made determination of the actual diameter impossible.

To eliminate these problems and obtain an undistorted view of the tube and the liquid, it was decided to provide a flat plane through which to view the meniscus. The conical surface could be created inside a solid piece of glass with a flat front surface. The method, which is explained in more detail in Appendix E, involves drilling through a piece of glass with straight and tapered diamond bits to create a rough conical hole in glass. The surfaces are then polished with a series of diamond pastes to produce a smooth and transparent surface free from visible defects. Using this method on a test piece, the liquid and meniscus could be seen clearly under magnification. Several sections, approximately 20mm in length, were cut from solid 12mm diameter Pyrex rods. Pyrex glass was chosen for the material because it would be more dimensionally stable under the stresses of grinding and polishing than conventional glass. It was planned to keep the diameter of the three-phase interphase less than 5mm. The 12mm diameter glass rod would be adequate for a tube of this size and still provide stock for strength. The maximum tube length required for a three-phase diameter of 5mm based on

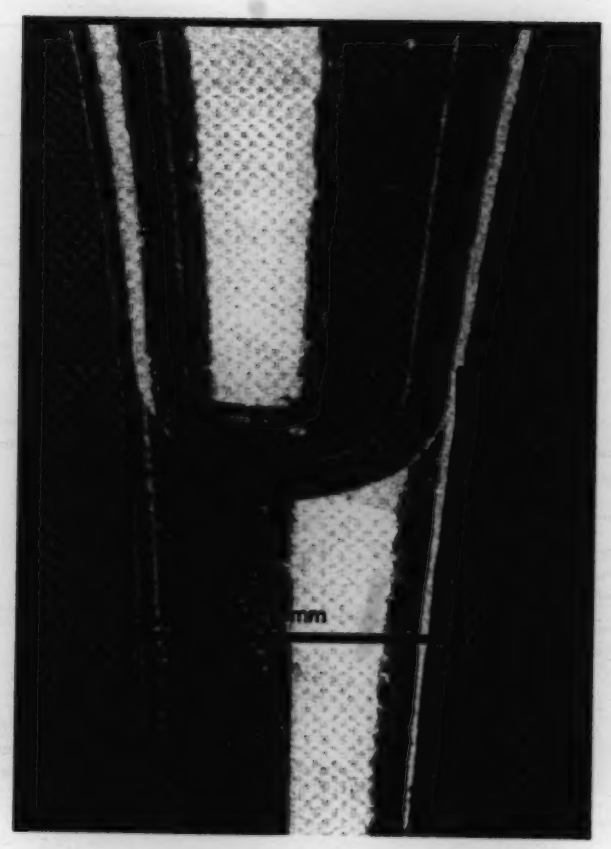

Figure 2.1: Drawn tube with capillary rise of water

Equation 1.38 was such that the tube length of 20mm was more than adequate. The flat viewing surface for the tube was ground and polished on the glass rod prior to creating the conical surface inside. Figure 2.2 is a sketch of a typical tube used in the experiment. The included angle for the created cone varied from tube to tube and ranged from approximately 12.6° to 16.8°. The angles that were created were largely controlled by the angle of the tapered diamond bit and the extent that the axis of the bit was inclined to the axis of the glass rod during grinding. Grinding and polishing to the final state determined the resulting cone angle.

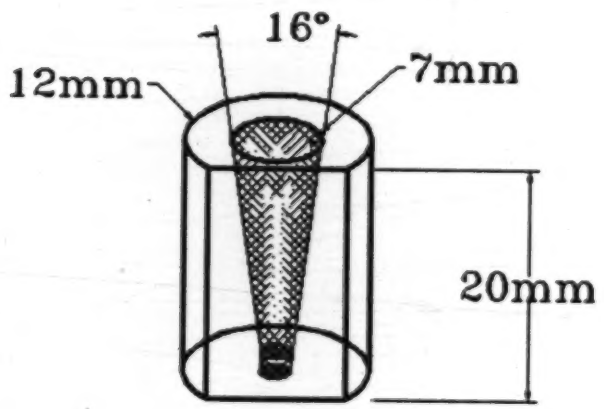

Figure 2.2: Sketch of conical capillary tube in glass rod

After polishing, the internal tube wall angle, from which β is derived, was measured with a toolmakers microscope to a resolution of 0.01 degrees and a repeatability of 0.04 degrees. Three tubes were created with internal angles of 12.80, 14.70 and 17.04 degrees. Each tube could potentially be used in the configuration shown in Figure 1.2 or inverted, resulting in 6 possible β angles for use. These tests used $\beta \triangleq 1.459$, 1.422, 1.443, and 1.682 where β is measured in radians.

2.3 Measurement apparatus

Having created a tube that would display a measurable meniscus, an apparatus was needed that would position and manipulate the tube in the liquid and enable the measurement of the three-phase diameter, and hence R, and the capillary rise H. A stereo microscope with changeable magnification was made available. Interchangeable eyepieces with graduated markings were also used. The concept was to essentially fix the microscope and manipulate the capillary tube and the chemical resevoir. The tube and reservoir would then be moved together, without disturbing the equilibrium, across the field of view of the microscope and a dial gauge would indicate the translation distance which would correspond to the three-phase diameter. Similarly the tube and reservoir would be lowered and raised, while being viewed through the microscope, so that the heights of the free surface and the three-phase meniscus could be recorded from another dial gauge. This would give the capillary height H.

The microscope was mounted at one end of an optical rail and the tube/reservoir assembly was mounted at the opposite end as shown in Figure 2.3

Several adjustments were necessary at the tube assembly end of the rail since the microscope itself remained stationary once focused and the tube and assembly moved relative to it when required. Referring to Figure 2.4; one positioner was needed to move the base, which supported the liquid reservoir and tube up and down along Y, a vertical axis. The dial indicator, labeled 'A', displayed vertical translations.

A second positioner enabled the base to be moved horizontally, along the X axis as displayed by the dial indicator labeled 'B'. Other positioners were used to move and rotate the tube relative to this $X-Y$ system or frame of reference. Positioners were used to move the tube horizontally and vertically along the x and y axis respectively. Leveling was achieved with the ability to rotate around two perpendicular axes. Only one axis is shown in Figure 2.4 for clarity. The tubes are held in a modified tube clamp as shown in Figure 2.5 allowing the tubes to be quicky secured and removed after use.

To obtain measurements the tube is first moved along the x axis until it can be seen through the microscope. It is then leveled in two

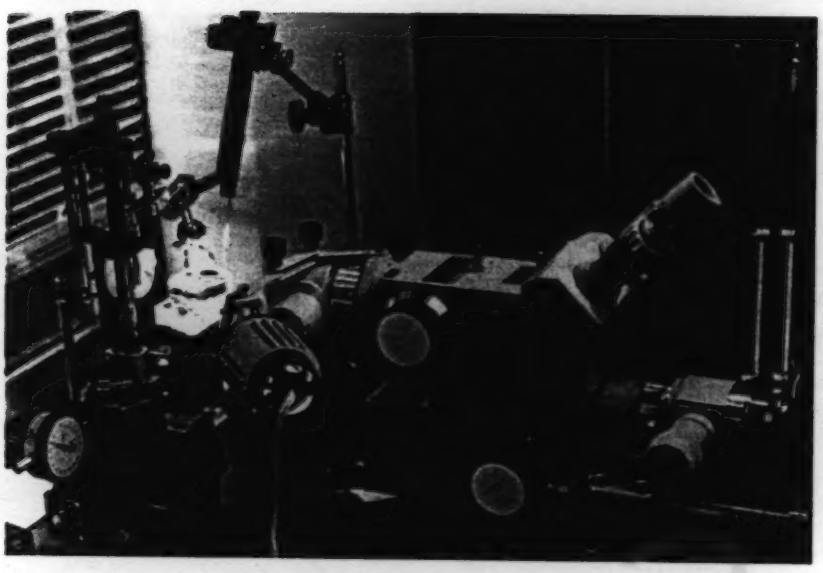

Figure 2.3: Measurement equipment

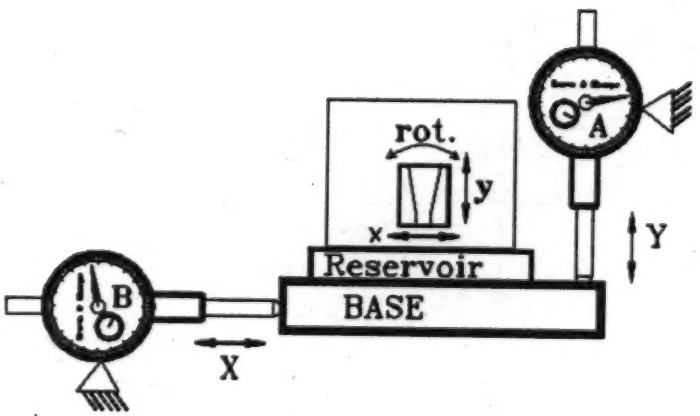

Figure 2.4: Measurement apparatus

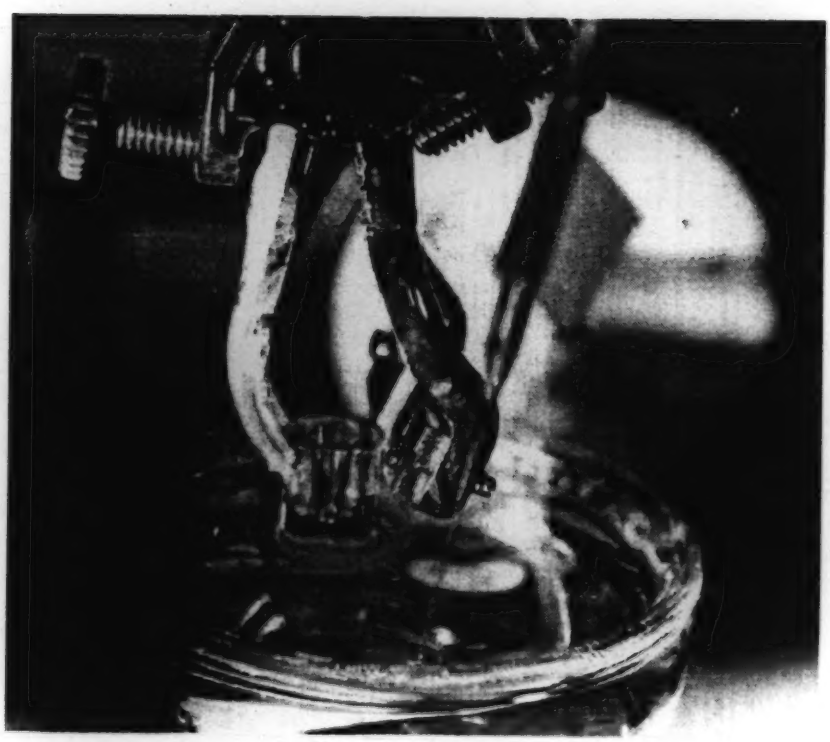

Figure 2.5: Modified tube clamp

axes and lowered along the y axis into the liquid reservoir until a visible meniscus forms. Refering to figure 2.6, the base, supporting the tube and reservoir, are moved along the X and Y axis until pt1 is coincident with a particular marking on the graduated scale when viewed through the microscope. At this point, the readings from both dial gauges are recorded. The base is moved horizontally along the X axis only, until pt2 is coincident with the same mark in the microscope view. If the point pt2 is not at the same vertical level the process is repeated. When it is at the same vertical level we can assume that the three-phase contact region is circular and level. The readings from both dial gauges are again taken at point pt2. The base is then moved up along axis Y until the free surface, point pt3, is coincident with the same mark in the microscope view. The three-phase diameter, D, is calculated as the difference in the horizontal dial gauge readings from pt1 to pt2. The capillary height H is calculated as the difference in the vertical dial gauge readings from pt2 to pt3.

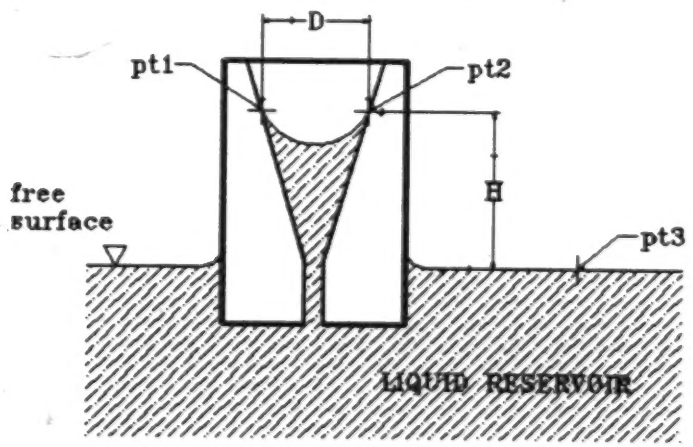

Figure 2.6: Cross section of tube in reservoir

Finding the free surface of the liquid reservoir corresponding to pt3 was not as simple as finding points pt1 or pt2. The most accurate and repeatable method that was tried and adopted was to use the reflection of a sharp point on the free surface. A glass fiber with a

sharp point was adjusted independently up or down until the point at the end was level with the same graduation marking aligned with points pt1 and pt2. The reservoir was raised until the point and its reflection, were both in the view of the microscope. The free surface was the line or point at the middle of the fiber tip and its reflection. Since a meniscus around the fiber would form if the tip touched the surface, the tip was suspended above the surface. The graduations in the eyepieces were calibrated and used to determine the remaining distance to the free surface. This being half the distance between the images. The base and hence the reflection, could be raised such that image and reflection were exactly one or two divisions apart. This was accurate and repeatable to the resolution of the dial gauge.

2.4 Calibration

The two dial gauges used to measure the three-phase diameter D and the capillary rise H had graduations of 0.001mm and 0.01mm respectively. It was possible to read the latter to 0.003 mm by visually dividing the distance between dial gauge markings into three zones and determining which zone the needle of the dial gauge rested in.

The 250X magnification and the graduations on the eye-piece were such that the distance between graduations in the microscope view , which were distinguishable, was $10\mu m$ or 0.010mm. A distinction could be made between positions representing the limits of the measuring resolution.

Resolution is critical in trying to measure such a small surface property as line tension, but even infinite resolution is useless if accurate measurements are not obtained. To test the accuracy of the system used for collecting data, a 4 mm gauge block was used to calibrate both vertical and horizontal measurements. 4mm represents the range of measurements for the three-phase diameter D and for all but one measurement of H. When the block was properly set up measurements for both the vertical and horizontal dial gauges were accurate and repeatable to the resolution stated above.

Possible distortion or magnification of the image from the tube was also checked. A metal cylinder, approximately 3 mm in diameter, was measured and then seated in the tube. When the cylinder was re-measured, no measureable distortion was noted.

2.5 System accuracy

Having determined the capillary tube dimensions and the ability of the measurement system to collect data, it was necessary to determine if the system was accurate enough to be used for the application. Two methods were used to estimate the accuracy of the experiment based on the two methods of determining line tension described above. Appendix B shows the calculations for a typical measurement using dodecane. The initial purpose for the analysis was to determine the magnitude of the probable error in line tension in relation to the value of line tension itself. It was hoped that the probable error would be an order of magnitude less than line tension.

For the curve fitting method, $\cos\theta$ and $\cos\beta/R$ were evaluated and the uncertainty or probable error for each was calculated from the partial derivatives of each. The estimated uncertainty for both $\cos\beta/R$ was significantly less than 1%. These values would change slightly for different capillary rises in other tubes with different liquids, but they do validate the method since the relative error for each is small. It would be expected that any significant deviations from linearity in the plot would be due to surface imperfections or other factors that would prevent the liquid from reaching the theoretical equilibrium height, rather than the inability to measure the geometry.

The error analysis using Equation 1.38 involves the uncertainty of $\cos\theta_\infty$ in addition to all of the parameters involved in the curve fitting method. The calculations for probable error in line tension using this method are also included in Appendix B. The value of $\cos\theta$ for an infinitely large three-phase contact radius is $\cos\theta_\infty$. Data for this point is outside of the measured range for this experiment or any experiment involving sessile drops and the drop size dependance on contact angle. $\cos\theta_\infty$ is an extrapolated value from a curve fitting relationship. It was therefore likely that the uncertainly in θ_∞ could be as much as several degrees. From an inspection of Equation 1.37 one would expect that uncertainty in line tension would be as sensitive to θ_∞ as it would be to the contact angle θ. As Li [2] explains, for procedures involving drop size dependance of contact angles for sessile drops, an error in contact angle of $\pm 2°$ is not acceptable. It is reasonable to assume then, that errors in

$\cos\theta_\infty$ of $\pm 2°$ are not acceptable either.

The sensitivity of line tension, as calculated by Equation 1.38 to uncertainly in $\cos\theta_\infty$ can be expressed by Equation 2.4

$$\frac{\partial\sigma}{\partial\theta_\infty} = \frac{-R\gamma_{lv}\sin\theta_\infty}{\cos\beta} \tag{2.4}$$

and the uncertainty in $\cos\theta$ can be expressed by Equation 2.5

$$\frac{\partial\sigma}{\partial\theta} = \frac{R\gamma_{lv}\sin\theta_\infty}{\cos\beta} \tag{2.5}$$

Equations 2.4 and 2.5 show that line tension accuracy is equally sensitive to errors in the equilibrium contact angle as it is to the extrapolated value of θ_∞. For the sample calculation in Appendix B, using measured data, the probable error in line tension for uncertainty in θ of only 1° is $3\mu Jm^{-1}$.

The probable error in the contact angle is also calculated in Appendix B using Equation 2.6 which is used to calculate intermediate values in the curve fitting analysis.

$$\theta = \beta - \arcsin\left[\frac{\Delta\rho g H R}{2\gamma_{lv}}\right] \tag{2.6}$$

This results in an uncertainty or probable error of less than 0.1 degree for typical values used in this test. Comparison of the error contribution of $\cos\theta$ and $\cos\theta_\infty$ would suggest that the line tension should be determined from the curve fitting method as opposed to using the direct method of substituting all variables including $\cos\theta_\infty$ into Equation 1.38.

Chapter 3

Results and Discussion

3.1 Initial test results

After the tubes and measuring apparatus were built and assembled, data collection proceeded rapidly. The results for the measured three-phase diameter and the capillary height H are shown in tabular form in Appendix A. Also shown in those tables are the values for $\cos\beta/R$ and $\cos\theta$. These are referred to as intermediate calculations as they are used in determining a linear relationship from which the line tension is derived. For the first set of tubes that were made and used in the experiment, it was noticed that the meniscus would not always move up the tube when the tube was lowered for the next reading. For a theoretically perfect tube and surface, the liquid should re-establish for even the most subtle change in equilibrium conditions, although the change may not be immediate. For this first set of tubes however, lowering the tube as much as $1mm$ did not produce a change. This would imply that the surface was not as smooth and homogenous as it should be. This created an additional limitation in the number of points or measurements that could be taken per tube before the meniscus reached the top of the tube.

When the data was analyzed for the first trials with the first tube, values for line tension using Equation 1.38 were calculated. The values of line tension were not the same for each measurement but all were between the values of 2 and 5 μJm^{-1}. The tests were initially deemed to be successful. When other tubes were tried with the same chemical, and even when the same tube was re-used, the results were

not consistent. The mean value would change, often by as much as $5\mu Jm^{-1}$ and the range of values would increase significantly. For many of these tests it appeared that the value of line tension would increase as the three-phase diameter increased. It was thought that the cause of this might be that the value of $\cos\theta_\infty$ used in Equation 1.38 was too large.

Figure 3.1 shows the effect an over-estimate of $\cos\theta_\infty$ may have on the calculated value of line tension if only one measured data point is used. The figure shows $l1$ drawn through a correct value of $\cos\theta_\infty$ and lines $l2$, $l3$, $l4$ drawn through an over-estimate of $\cos\theta_\infty$. Observing lines $l2$ to $l4$ it can be seen that the magnitude of the slope increases with the radius R. The line $l1$ passes through all of the points and hence the slope from the correct value of $\cos\theta_\infty$ to any point is constant.

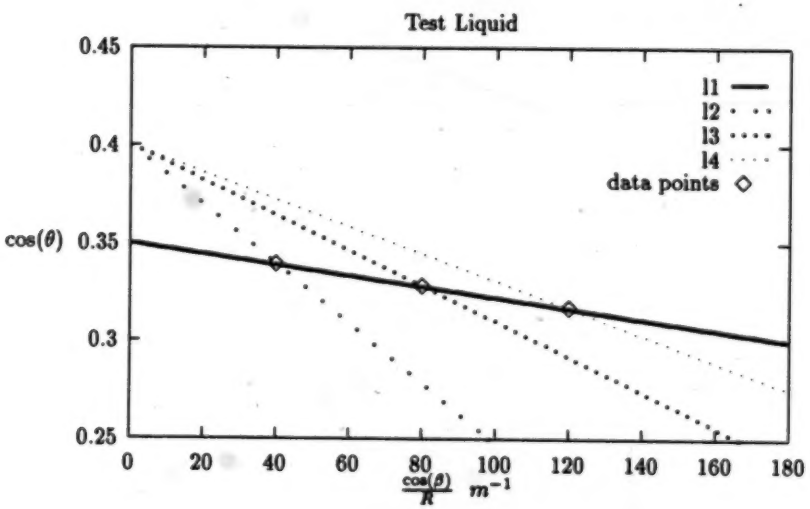

Figure 3.1: Possible errors in assumption of $\cos\theta_\infty$

It is apparent that the opposite trend would appear if the value of $\cos\theta_\infty$ was under-estimated. This was thought to be the explanation for the apparent increase in line tension values for larger values of R in some of the initial tests. It was thought that the value for $\cos\theta_\infty$ was an over-estimation for our system.

If all of the coordinates, $\cos\beta/R$ and $\cos\theta$ were plotted for a given chemical, a linear relationship should be apparent, from which we could calculate $\cos\theta_\infty$ and more importantly line tension, σ. Figure 3.2 is the product from plotting all the calculated values for decane from multiple tests using all of the tubes.

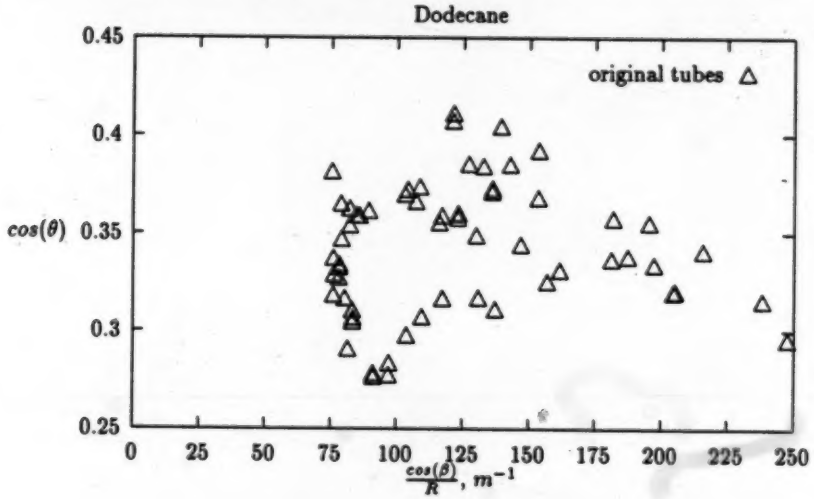

Figure 3.2: Results from original polishing

The results of others, which indicate that there is no relationship between contact angle $\cos\theta$ and drop size R, or conclude that line tension is negative, might seem to be valid in light of Figure 3.2. Using selected points, any or no relationship could be drawn.

Li [1] explains that this scatter develops because the surface was not smooth, homogenous and free from defects even though care was taken in manufacturing and coating the tubes. From the initial estimates of uncertainty, it is clear that the distribution shown is not the result of an inability to measure the necessary parameters. When the tubes were re-examined under the microscope at higher resolution, small defects were apparent. Many attempts were made to remove the defects by re-polishing the surface, without success.

3.2 Re-polished tubes

Barry Arnold of the Technical Services department at the University of Alberta whose expertise was in lens manufacturing was requested to finish the polishing on the tubes to bring them to optical quality.

Mr. Arnold used a lathe to turn an aluminum rod for use as a polishing tool. It was turned to the same angle as the conical capillary tube to avoid creating a non-linear wall or one with waves. This tool would spin inside the tube, while being surrounded by a polishing slurry. The tube was also spun in an opposite direction to develop an evenly polished surface. An aluminum oxide water slurry was used for about 10 minutes to create a uniform surface defect level of 12μ. At this point the glass was still frosted. The process was repeated with a finer slurry which produced a surface defect level of 9μ. A new aluminum rod had to be made for each change of slurry grade. A final rod was turned and covered in a polishing pitch made from C_e0_2 and warm water. After 20 minutes of polishing while keeping the surface wet with slurry, the surface was finished. A surface smoothness or defect level of $10A°$ was then obtained on the surface as reported by Mr Arnold.

When these re-polished tubes were used, the meniscus moved smoothly from equilibrium to equilibrium. The meniscus responded to smaller movements of the tube into the liquid reservoir, allowing many more samples points to be taken per tube. The plotted results with the calculated linear regression curves are shown in Figure 3.3 - Figure 3.6 for the four chemicals tested.

Each figure, including Figure 3.2, uses approximately the same scale so as not to distort the results relative to each other. It is immediately apparent that extremely careful surface preparation has significantly reduced the variance of the values from a linear relationship. In light of the previous tests, the glass surface must have been the dominant factor in this variance. The results shown in these figures are summarized in Table 3.1.

The sample correlation coefficient r is often used as an indicator of the strength of a linear relationship derived from sample data. The value of r is defined such that it can assume a value between $+1$ and -1. A negative value would indicate that as one variable increases, the other decreases. A negative correlation should be expected for this experiment. The coefficient of determination, r^2, is

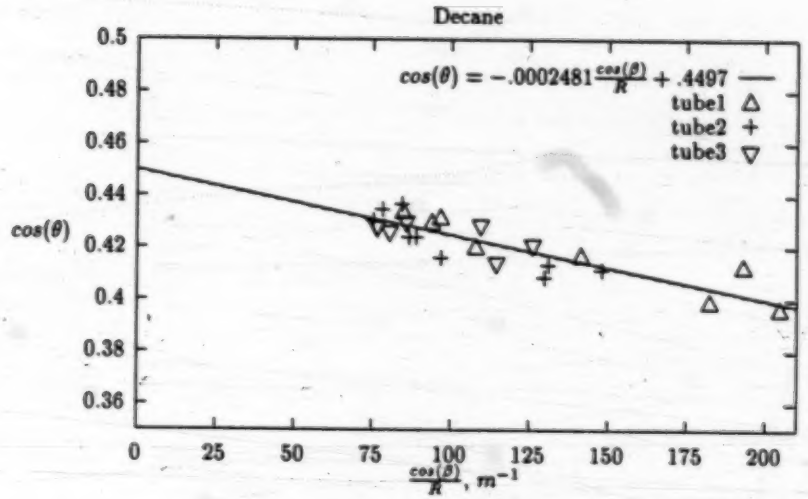

Figure 3.3: Results from decane

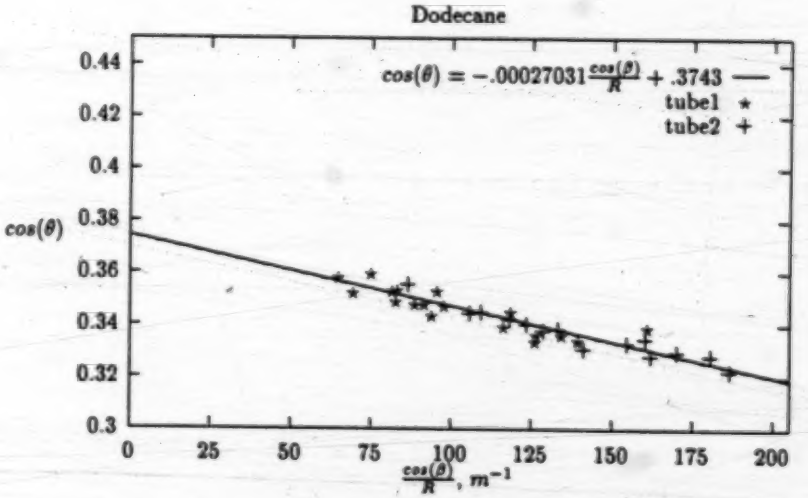

Figure 3.4: Results from dodecane

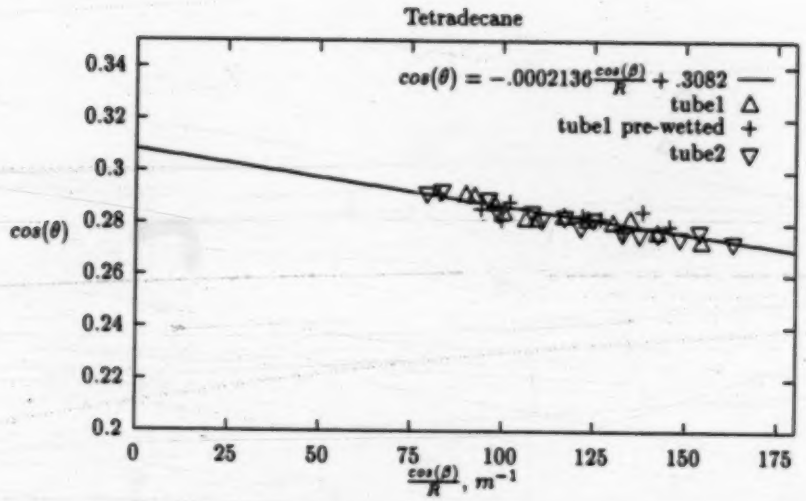

Figure 3.5: Results from tetradecane

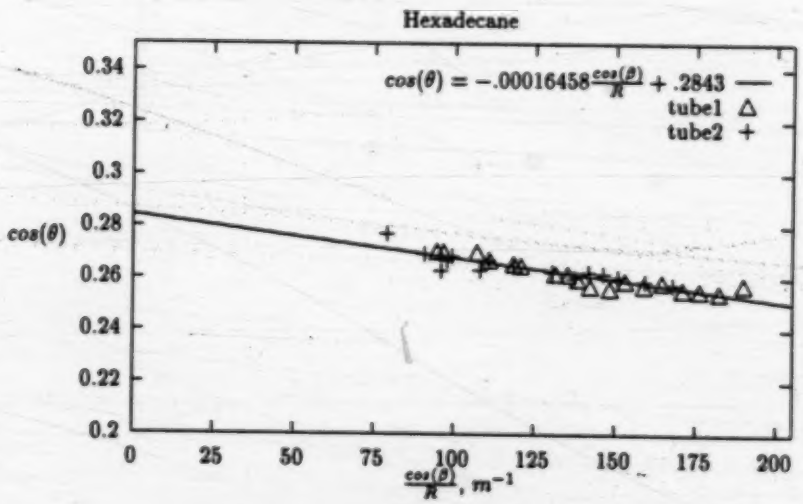

Figure 3.6: Results from hexadecane

Table 3.1: Calculated results from $\cos\theta$ vs $\cos\beta/R$

Liquid	Line tension σ (μJm^{-1})	θ_∞ degrees	Correlation coefficient r	Coefficient of determination r^2
Decane	5.8 ±1.5	62.3 ±.5	-0.87	0.76
Dodecane	6.8 ±.9	68.0 ±.3	-0.94	0.88
Tetradecane	5.7 ±.9	72.0 ±.3	-0.90	0.81
Hexadecane	4.5 ±.8	73.5 ±.2	-0.91	0.83

the proportion of the variation of the one variable that is determined by the variation in the other[39], and hence is a more informative statistic. The value of $100r^2$ is the percent of the variation of $\cos\theta$ that is attributed to a variation in $\cos\beta/R$. For the worst case of the four chemicals tested, we find that 76% of the variance in $\cos\theta$ can be explained by the variance in the size of the three-phase contact radius, or more exactly, $\cos\beta/R$. The unaccounted variance from other sources would then account for only 24%. For dodecane, which has the best correlation, we find that there is only 12% unexplained variance. This unexplained variance would include the effects of surface preparation and other factors not included in this discussion. Table 3.2 shows the results that were obtained by D. Duncan et al. using an ADSA technique on drop size dependance on contact angle [9] and a method using similar equipment on solid cones or frustums by Y. Gu et. al. [34].

Table 3.2: Comparitive results from ADSA and ACRPAC techniques

Liquid	Line tension σ (μJm^{-1})	θ_∞ degrees	Correlation coefficient r	Solid Surface
Decane [a]	1.7	58.5	0.85	FC725
Decane [b]	1.9	65.5	-	FC721
Dodecane[a]	2.1	69.6	0.91	FC725
Dodecane[b]	2.1	69.6	-	FC721
Tetradecane[a]	3.3	65.4	0.84	FC725
Hexadecane[a]	3.7	69.5	0.83	FC725

[a]Ref.[34]
[b]Ref.[9]

Although both FC721 and FC725 are cited in Table 3.2, the two coatings are both excellent hydrophobic surfaces with low surface energies, and are very similar to FC722 and as such the values ob-

tained can be used for comparison purposes.

The first thing to notice regarding the correlation coefficients is that Gu et. al. [34] reports positive values. This should not be regarded as an opposite trend but a convention chosen by him for reporting. The values of r reported by Gu et. al. correspond closely with those from the conical capillary tube method, although somewhat lower for each chemical. If a comparison is to be made, the values of r^2 should be compared. This evaluation would show as much as a 14% better correlation for the conical capillary tube method. Correlation values are not included for the results for Duncan et. al. [9] because values are given for each of several runs and would not be a suitable comparison to the method described here which uses the correlation coefficient from data collected over multiple runs.

A difference in the values for θ_∞ from Tables 3.2 and 3.1 is as much as 6.6° and even the closest comparison varies by 1.6°. If the method for calculating line tension from a single measurement were used, as described in the introduction, the value of θ_∞ from an alternate source would have to be included. From the comparison above, it is apparent that this could introduce significant errors. The sample calculations that are included in Appendix B show for a typical example using dodecane that the smallest difference from above of 1.6° could introduce an error of $4.7\mu Jm^{-1}$, which is almost as large as the value of line tension itself. Initial tests that calculated line tension from a single measurement seemed to be flawed from tube preparation, but the value of θ_∞ was 1.6° higher than that obtained from the a curve analysis. This could partially explain the observed trend of increasing line tension with contact radius in inital tests. It should be recalled that this error generated from an over or under-estimate of θ_∞ depends on the contact radius and can become even more significant. Clearly, it is desirable to eliminate the probable error introduced from assuming a value of θ_∞ from a previous study.

The results summarized in Table 3.1 are from the linear regression analysis of multiple measurements and as such do not require the input of θ_∞. Although a confidence interval is shown for θ_∞ it must be stressed that this point is not within the range of data measured and that the values stated should only be used for comparison to similarly extrapolated values.

The values of line tension shown are all positive and are of the

order of $1\mu Jm^{-1}$. All the tested liquids were from the decane family and hence is not surprising that the values for line tension are similar. The range in values of $2.3\mu Jm^{-1}$ compares to the range of $2.0\mu Jm^{-1}$ reported by Gu et. al. [34]. It can be seen that for all the chemicals tested, the confidence interval for line tension values is less than $\pm 1.5\mu Jm^{-1}$ for all tests and less than $\pm 1\mu Jm^{-1}$ for three of the four chemicals. The uncertainty or confidence interval equates, for these tests, to a maximum of 26% of the value of line tension. It was hoped that the uncertainty would be an order of magnitude less, or 10% of line tension. Although this was not obtained, the curve with the best correlation provided an uncertainty of 13%. For both θ_∞, and σ, the uncertainty or $\pm$ values are calculated at a 95% confidence limit based on the distribution of measured data.

Chapter 4

Conclusions

A simple conical capillary tube can be used to evaluate line tension with a 95% confidence interval significantly less than the value of the line tension itself. The method requires that two measurements are taken for each of several capillary rises and that line tension be derived from a linear regression analysis of calculated results using $\cos\beta/R$ vs $\cos\theta$.

For the liquids from the decane family tested as part of this research, ie. decane, dodecane, tetradecane and hexadecane, the values of line tension range from 4.5 to 6.8 μJm^{-1}. The results support recent theoretical analysis showing that line tension is a positive quantity, and also recent experimental work showing that line tension is positive and of the order of $1\mu Jm^{-1}$.

This unique approach to measuring line tension is simple. The data collected consists of measuring the distance from the top of a capillary rise to the liquid reservior free surface and the formed meniscus diameter using dial gauges and a microscope. The equipment, other than the glass conical capillary tubes, are either readily available or easily built or adapted. Careful preparation of the glass surface is critical in obtaining useful results. The surface must be smooth and free of defects at a microscopic level and the tube wall angle must be constant over the range tested. The surface coatings must have a low surface energy and form a smooth homogenous surface free of defects and not react with the chemicals tested. In addition the tube must be manufactured such that the meniscus is clearly visible without distortion and can be easily identified.

Since this method is simple, cost effective and accurate, it is ex-

pected and hoped that it will be applied to other chemicals and chemical families to determine line tension values. Other experiments showing negative values for line tension, or no correlation in the analysis, could be redone using the conical capillary tube at a minimum cost. With proper tube preparation these too should also show an excellent correlation, supporting this research into the sign and magnitude of line tension.

Appendix A

Tabular data

Table A.1: Properties used in calculations

Liquid	Chemical Formula	Mol Wgt. g/mol	$\Delta\rho$ (kg/m^3)	γ_{lv} (mJ/m)
Decane	$C_{10}H_{22}$	144	727	23.43
Dodecane	$C_{12}H_{26}$	170	748	25.44
Tetradecane	$C_{14}H_{30}$	196	762.8	26.7
Hexadecane	$C_{16}H_{34}$	222	773	27.6

Table A.2: Decane measured data and calculated intermediate results

Diam. (mm)	height (mm)	$\cos(\beta)/R$	$\cos(\theta)$
Capillary angle $\beta = 1.422$			
1.448	2.323	204.8	0.3968
2.093	1.742	141.7	0.4171
2.744	1.346	108.1	0.4206
3.059	1.258	96.93	0.4317
3.153	1.212	94.04	0.4298
3.486	1.113	85.05	0.4340
1.534	2.339	193.3	0.4130
1.625	2.092	182.5	0.3994
Capillary angle $\beta = 1.682$			
2.942	2.355	75.44	0.4305
2.830	2.467	78.43	0.4348
2.622	2.672	84.65	0.4367
2.556	2.680	86.83	0.4241
2.491	2.750	89.10	0.4241
2.286	2.953	97.09	0.4160
1.707	3.900	130.0	0.4085
1.692	3.970	131.2	0.4134
1.497	4.472	148.3	0.4115
Capillary angle $\beta = 1.443$			
2.020	1.968	126.2	0.4219
2.324	1.755	109.7	0.4294
2.222	1.747	114.7	0.4151
2.962	1.383	86.06	0.4307
3.161	1.280	80.64	0.4270
3.327	1.225	76.61	0.4292
3.322	1.225	76.76	0.4287

Table A.3: Dodecane measured data and calculated intermediate results

Diam. (mm)	height (mm)	$\cos(\beta)/R$	$\cos(\theta)$
Capillary angle $\beta = 1.459$			
2.720	2.320	81.65	0.3534
2.665	2.370	83.33	0.3538
2.270	2.747	97.83	0.3477
1.762	3.438	126.0	0.3343
1.386	2.324	161.0	0.3393
1.601	1.970	139.4	0.3347
1.660	1.917	134.4	0.3366
1.764	1.805	126.5	0.3367
1.884	1.757	118.4	0.3455
1.919	1.682	116.3	0.3398
2.333	1.467	95.64	0.3534
2.378	1.383	93.83	0.3440
2.437	1.375	91.56	0.3484
2.515	1.333	88.72	0.3485
2.697	1.248	82.73	0.3494
2.973	1.184	75.05	0.3601
3.213	1.063	69.45	0.3529
3.434	1.019	64.98	0.3587
Capillary angle $\beta = 1.443$			
1.366	2.020	186.6	0.3223
1.410	2.017	180.8	0.3281
1.497	1.914	170.3	0.3296
1.572	1.810	162.1	0.3282
1.647	1.769	154.8	0.3330
1.588	1.850	160.5	0.3347
1.805	1.598	141.2	0.3310
1.911	1.565	133.4	0.3384
1.979	1.507	128.8	0.3378
2.063	1.463	123.6	0.3403
2.153	1.415	118.4	0.3422
2.328	1.325	109.5	0.3449
2.406	1.280	105.9	0.3445

Table A.4: Tetradecane measured data and calculated intermediate results

Diam. (mm)	height (mm)	$cos(\beta)/R$	$cos(\theta)$
Capillary angle $\beta = 1.459$			
1.444	1.623	154.5	0.2732
1.566	1.530	142.5	0.2768
1.651	1.496	135.1	0.2819
1.710	1.433	130.5	0.2805
1.806	1.367	123.5	0.2818
1.906	1.305	117.1	0.2830
2.038	1.213	109.5	0.2820
2.090	1.182	106.8	0.2819
2.217	1.132	100.6	0.2846
2.276	1.125	98.03	0.2880
2.408	1.080	92.66	0.2908
2.473	1.055	90.22	0.2913
Capillary angle $\beta = 1.459$(prewetted)			
1.530	1.588	145.8	0.2791
1.610	1.560	138.6	0.2847
1.674	1.434	133.3	0.2771
1.756	1.408	127.1	0.2820
1.828	1.360	122.1	0.2830
2.182	1.175	102.3	0.2883
2.229	1.105	100.1	0.2814
2.363	1.068	94.43	0.2855
2.689	0.970	82.98	0.2913
Capillary angle $\beta = 1.443$			
1.563	1.360	163.1	0.2738
1.655	1.322	154.0	0.2780
1.715	1.255	148.7	0.2756
1.787	1.218	142.6	0.2772
1.851	1.173	137.7	0.2769
1.916	1.138	133.0	0.2775
2.038	1.109	125.1	0.2829
2.094	1.057	121.7	0.2797
2.174	1.045	117.5	0.2837
2.296	0.982	111.0	0.2825
2.254	0.975	108.3	0.2853
2.569	0.893	99.22	0.2852
2.643	0.897	96.44	0.2904
3.044	0.793	83.74	0.2934
3.198	0.750	79.71	0.2923

Table A.5: Hexadecane measured data and calculated intermediate results

Diam. (mm)	height (mm)	$\cos(\beta)/R$	$cos(\theta)$
Capillary angle $\beta = 1.422$			
1.560	1.038	190.0	0.2573
1.626	0.968	182.3	0.2543
1.682	0.943	176.3	0.2551
1.733	0.918	171.1	0.2554
1.801	0.907	164.6	0.2583
1.864	0.865	159.1	0.2569
1.935	0.848	153.2	0.2588
1.997	0.800	148.5	0.2559
2.082	0.773	142.4	0.2566
2.139	0.772	138.6	0.2595
2.188	0.768	135.5	0.2614
2.251	0.748	131.7	0.2616
2.453	0.705	120.9	0.2647
2.499	0.696	118.7	0.2653
2.667	0.660	111.2	0.2667
2.766	0.652	107.2	0.2696
3.063	0.590	96.80	0.2699
3.131	0.578	94.70	0.2700
Capillary angle $\beta = 1.443$			
1.516	1.270	168.1	0.2575
1.598	1.218	159.5	0.2589
1.688	1.168	151.0	0.2606
1.739	1.143	146.6	0.2617
1.796	1.113	141.9	0.2624
1.855	1.060	137.4	0.2602
1.951	1.025	130.6	0.2625
2.152	0.945	118.4	0.2647
2.300	0.898	110.8	0.2669
2.355	0.853	108.2	0.2631
2.564	0.815	99.41	0.2685
2.604	0.792	97.89	0.2667
2.653	0.755	96.08	0.2627
2.807	0.749	90.81	0.2693
3.220	0.688	79.16	0.2769

Appendix B

Sample Calculations

From Equation 1.36 we can express θ as

$$\theta = \beta - \arcsin \nu \tag{B.1}$$

To simplify subsequent calculations

$$\nu = \frac{\Delta \rho g H R}{2\gamma_{lv}}$$

The line tension, σ, can be expressed as

$$\sigma = \frac{\cos\theta_\infty - \cos\theta}{\cos\beta} R\gamma_{lv} \tag{B.2}$$

The partial derivatives, $\frac{\partial\theta}{\partial R}$, $\frac{\partial\theta}{\partial H}$, and $\frac{\partial\theta}{\partial\beta}$ are useful in error analysis and can be derived as:

$$\begin{aligned} \frac{\partial\theta}{\partial R} &= -\frac{\partial}{\partial\nu}\arcsin\nu\frac{\partial\nu}{\partial R} \\ &= -\left(\frac{1}{\sqrt{1-\nu^2}}\right)\frac{\nu}{R} \end{aligned} \tag{B.3}$$

(B.4)

$$\begin{aligned} \frac{\partial\theta}{\partial H} &= -\frac{\partial}{\partial\nu}\arcsin\nu\frac{\partial\nu}{\partial H} \\ &= -\left(\frac{1}{\sqrt{1-\nu^2}}\right)\frac{\nu}{H} \end{aligned} \tag{B.5}$$

(B.6)

$$\frac{\partial \theta}{\partial \beta} = 1 \tag{B.7}$$

The partial derivatives for ρ or ρg are not included here since they can be determined to several decimal places and are known from published data given for the temperature at which the experimental data was taken. The possible error in γ_{lv} was also neglected since the values obtained from experiments using ADSA are accurate to $\pm 0.01 mJm^{-2}$. The partial derivatives, $\frac{\partial \sigma}{\partial \beta}$, $\frac{\partial \sigma}{\partial R}$, $\frac{\partial \sigma}{\partial H}$, can then be derived as follows:

$$\begin{aligned}
\frac{\partial \sigma}{\partial \beta} &= [(\cos\theta_\infty - \cos\theta)\frac{\partial}{\partial \beta}\sec\beta + \sec\beta\frac{\partial}{\partial \beta}(\cos\theta_\infty - \cos\theta)]R\gamma_{lv} \\
&= [(\cos\theta_\infty - \cos\theta)\sec\beta\tan\beta - \sec\beta\sin\theta]R\gamma_{lv} \\
&= R\gamma_{lv}\sec\beta[(\cos\theta_\infty - \cos\theta)\tan\beta - \sin\theta]
\end{aligned} \tag{B.8}$$

$$\begin{aligned}
\frac{\partial \sigma}{\partial R} &= \left[\cos\theta_\infty - \cos\theta - R\frac{\partial \cos\theta}{\partial R}\right]\frac{\gamma_{lv}}{\cos\beta} \\
&= \left[\cos\theta_\infty - \cos\theta + R\sin\theta\frac{\partial \theta}{\partial R}\right]\frac{\gamma_{lv}}{\cos\beta} \\
&= \left[\cos\theta_\infty - \cos\theta + R\sin\theta\frac{\nu}{R}\left(\frac{1}{\sqrt{1-\nu^2}}\right)\right]\frac{\gamma_{lv}}{\cos\beta}
\end{aligned} \tag{B.9}$$

$$\begin{aligned}
\frac{\partial \sigma}{\partial H} &= \frac{R\gamma_{lv}}{\cos\beta}\sin\theta\frac{\partial}{\partial \nu}\arcsin\nu\frac{\partial \nu}{\partial H} \\
&= \frac{R\gamma_{lv}}{\cos\beta}\sin\theta\left(\frac{1}{\sqrt{1-\nu^2}}\right)\frac{\nu}{H}
\end{aligned} \tag{B.10}$$

$$\frac{\partial \sigma}{\partial \theta_\infty} = \frac{-R\gamma_{lv}\sin\theta_\infty}{\cos\beta} \tag{B.11}$$

$$\frac{\partial \sigma}{\partial \theta} = \frac{R\gamma_{lv}\sin\theta_\infty}{\cos\beta} \tag{B.12}$$

Sample Calculations for an example taken from Dodecane

Table B.1: Values used in calculations

Variable	Value	Uncertainty	Units
3 phase Diam D	1.601	0.002	mm
Capillary Height H	1.970	0.003	mm
Wall Angle β	1.459	.000175	Rad
Density $\Delta\rho$	748		kg/m^3
Surface Tension γ_{lv}	25.44		mJ/m^2

ESTIMATE OF THE ERROR IN DERIVED VALUE OF $\cos\theta$

$$\begin{aligned} \nu &= \left[\frac{\Delta\rho g H R}{2\gamma_{lv}}\right] \\ &= \left[\frac{748 * 9.81 * 1.970 * 10^{-3} * 8.005 * 10^{-4}}{2 * 25.44 * 10^{-3}}\right] \\ &= .2247 \end{aligned} \tag{B.13}$$

$$\begin{aligned} \theta &= \beta - \arcsin\nu \\ &= 1.459 - \arcsin(.2247) \\ &= 1.2295 \end{aligned} \tag{B.14}$$

As an approximation of the error in θ, symbolized by $\epsilon\theta$ we shall use the parital derivatives presented earlier.

$$\epsilon\theta \simeq \sqrt{(\frac{\partial\theta}{\partial R}\epsilon R)^2 + (\frac{\partial\theta}{\partial H}\epsilon H)^2 + (\frac{\partial\theta}{\partial\beta}\epsilon\beta)^2} \tag{B.15}$$

$$\begin{aligned} \frac{\partial\theta}{\partial R} &= -\left(\frac{1}{\sqrt{1-\nu^2}}\right)\frac{\nu}{R} \\ &= -\left(\frac{1}{\sqrt{1-.2247^2}}\right)\frac{.2247}{8.005 * 10^{-4}} \\ &= -288.07 \end{aligned} \tag{B.16}$$

$$\epsilon R = 1 * 10^{-6} \tag{B.17}$$

$$\frac{\partial\theta}{\partial H} = -\left(\frac{1}{\sqrt{1-\nu^2}}\right)\frac{\nu}{H}$$

$$= -\left(\frac{1}{\sqrt{1-.2247^2}}\right)\frac{.2247}{1.790*10^{-3}}$$

$$= -117.05 \tag{B.18}$$

$$\epsilon H = 3*10^{-6} \tag{B.19}$$

$$\frac{\partial\theta}{\partial\beta} = 1 \tag{B.20}$$

$$\epsilon\beta = 0.000175 \tag{B.21}$$

$$\epsilon\theta \simeq \sqrt{(-288.07*1*10^{-6})^2+(-117.05*3*10^{-6})^2+.000175^2}$$

$$= 3.5680*10^{-4} \Rightarrow 0.02 degrees \tag{B.22}$$

ESTIMATION OF ERRORS IN COORDINATES FOR CURVE FITTING

X:$\frac{\cos\beta}{R}$

$$R = \frac{D}{2} = \frac{1.601*10^{-3}m}{2} = 8.005*10^{-4}$$

$$\cos(\beta) = \cos(1.459) = .11564 \tag{B.23}$$

$$\frac{\cos\beta}{R} = 139.37 = 139.4m^{-1} \tag{B.24}$$

Y:$\cos\theta$

$$\cos\theta = \cos(\beta - \arcsin\nu)$$

$$= \cos(1.459 - \arcsin(.2247))$$

$$= \cos(1.2295)$$

$$= 0.33465 = .3347 \tag{B.25}$$

ϵX : Error in X from β and R: ϵX_β and ϵX_R

$$\epsilon X_R \simeq |\frac{\partial}{\partial R}(\frac{\cos\beta}{R})dR|$$

$$= \frac{\cos\beta}{R^2}dR$$

$$dR = \frac{\epsilon D}{2} = \frac{2*10^{-6}m}{2} = 1*10^{-6}m$$

$$\epsilon X_R = \frac{\cos 1.459}{(8.005*10^{-4})^2}*10^{-6}$$

$$= .174m^{-1} \tag{B.26}$$

$$\begin{aligned}
\epsilon X_\beta &\simeq |\frac{\partial}{\partial\beta}(\frac{\cos\beta}{R})d\beta| \\
&= \frac{\sin\beta}{R}d\beta \\
&= \frac{\sin 1.459}{8.005 * 10^{-4}} * 1.75 * 10^{-4} \\
&= 0.217m^{-1} \qquad \text{(B.27)}
\end{aligned}$$

$$\begin{aligned}
\epsilon X &= \sqrt{(\epsilon X_\beta)^2 + (\epsilon X_R)^2} \\
&= .28m^{-1}
\end{aligned}$$

$$\frac{\epsilon X}{X} = \frac{.28}{139.4} = 0.2\% \qquad \text{(B.28)}$$

ϵY : Error in Y from β and H and R: ϵY_β and ϵY_H and ϵY_R

$$\begin{aligned}
\epsilon Y_R &\simeq |\frac{\partial}{\partial R}\cos\theta dR| \\
&= \sin\theta\frac{\partial\theta}{\partial R}dR \\
&= \sin(1.2295) * 288.07 * 10^{-6} \\
&= 0.00027 \qquad \text{(B.29)}
\end{aligned}$$

$$\begin{aligned}
\epsilon Y_H &= |\frac{\partial}{\partial H}(\cos\theta)dH| \\
&= \sin\theta\frac{\partial\theta}{\partial H}dH \\
&= sin(1.2295) * 117.05 * 3 * 10^{-6} \\
&= 0.00033 \qquad \text{(B.30)}
\end{aligned}$$

$$\begin{aligned}
\epsilon Y_\beta &= |\frac{\partial}{\partial\beta}(\cos\theta)d\beta| \\
&= \sin\theta d\beta \\
&= \sin(1.2295) * 1.75 * 10^{-4} = 0.00016 \qquad \text{(B.31)}
\end{aligned}$$

$$\begin{aligned} \epsilon Y &\simeq \sqrt{(\epsilon Y_R)^2 + (\epsilon Y_H)^2 + (\epsilon Y_\beta)^2} \\ &= \sqrt{(.00027)^2 + (.00033)^2 + (.00016)^2} \\ &= 0.00046 \\ \frac{\epsilon Y}{Y} = \frac{0.00046}{.3347} &= 0.14\% \end{aligned} \tag{B.32}$$

ESTIMATION OF ERROR USING SINGLE CAPILLARY MEASUREMENT

Possible error in σ using the numbers from a dodecane test result and an error in $\cos\theta_\infty$ of 1.6° or 0.028 rad . The error value of 1.6° was chosen as it represents the smallest difference in values of $\cos\theta_\infty$ obtained in this experiment and that reported by Li for Dodecane.

$$\begin{aligned} \frac{\partial\sigma}{\partial\theta_\infty} &= \frac{-R\gamma_{lv}\sin\theta_\infty}{\cos\beta} \\ &= \frac{-8.005 * 10^{-4} * 25.44 * 10^{-3} * \sin 1.18}{\cos 1.459} \\ &= -1.69 * 10^{-4} \end{aligned} \tag{B.33}$$

As an approximation to the error in line tension, $\epsilon\sigma$ as a result of an error in contact angle, $\epsilon\theta_\infty$

$$\begin{aligned} \epsilon\sigma &\simeq |\frac{\partial\sigma}{\partial\theta_\infty}| * \epsilon\theta_\infty \\ &= 1.69 * 10^{-4} * 0.028 \\ &= 4.7\mu Jm^{-1} \end{aligned} \tag{B.34}$$

For an error in θ_∞ of 1° the result is calulated as

$$\epsilon\sigma = 1.69 * 10^{-4} * 0.017 = 2.95\mu Jm^{-1} \tag{B.35}$$

Appendix C

Statistical analysis

In general, for a linear regression curve of y on x, the mean of the distribution of the y values is given by $\alpha+\beta x$ From the context of this discussion, β should not be confused with the angle of inclination for the sessile tube. y will in general, deviate from this mean, and we denote the difference as ϵ. The mean value of ϵ can be set to zero by an appropriate choice of α. The value of ϵ will depend on measurement errors and on other factors that cannot be directly measured.

The following expressions are useful in obtaining the equation $y = a + bx$ which is an estimate of the regression line $y = \alpha + \beta x$.

$$\begin{aligned} S_{xx} &= n\sum_{i=1}^{n} x_i^2 + \left(\sum_{i=1}^{n} x_i\right)^2 \\ S_{yy} &= n\sum_{i=1}^{n} y_i^2 + \left(\sum_{i=1}^{n} y_i\right)^2 \\ S_{xy} &= n\sum_{i=1}^{n} x_i y_i - \left(\sum_{i=1}^{n} x_i\right)\left(\sum_{i=1}^{n} y_i\right) \\ s_e^2 &= \frac{S_{xx}S_{yy} - S_{xy}^2}{n(n-2)S_{xx}} \end{aligned} \qquad \text{(C.1)}$$

Using this notation, a and b are solved as

$$a = \overline{y} - b\overline{x} \quad and \quad b = \frac{S_{xy}}{S_{xx}} \qquad \text{(C.2)}$$

where $\overline{y}$ = average y value, $\overline{x}$ = average x value. The confidence interval for α is constructed as

$$a \pm t_{\alpha/2} s_e \sqrt{\frac{S_{xx} + (n\overline{x})^2}{nS_{xx}}} \tag{C.3}$$

and the confidence interval limits for β are solved as

$$b \pm t_{\alpha/2} s_e \sqrt{\frac{n}{S_{xx}}} \tag{C.4}$$

Here the symbol α is used for both a parameter of the regression line and for the level of confidence. The context should be such that there is no confusion. There should also be no confusion with the use of β which is used in this context as a parameter of the regression and not the angle of inclination for the capillary tube.

The sample correlation coefficient is calculated as

$$r = \frac{S_{xy}}{\sqrt{S_{xx} \cdot S_{yy}}} \tag{C.5}$$

For the tests involving Dodecane, the following sample calculations illustrate the use of these statistical equations in solving for line tension and the confidence in that value.

Appendix D

Dodecane Statistical Calculations

$$
\begin{aligned}
n &= 31 \quad \sum_{i=1}^{n} x_i = 3722.63 \quad \sum_{i=1}^{n} y_i = 10.5923 \\
\overline{x} &= 120.085 \quad \overline{y} = .3417 \\
\sum_{i=1}^{n} x_i^2 &= 481067.9 \quad \sum_{i=1}^{n} y_i^2 = 3.6222 \quad \sum_{i=1}^{n} x_i y_i = 1262.93
\end{aligned} \tag{D.1}
$$

Substituting Equation D.1 into Equations C.1 results in

$$
\begin{aligned}
S_{xx} &= 1055130 \quad S_{yy} = 0.08443 \\
S_{xy} &= -280.391 \quad s_e^2 = 1.10294 * 10^{-5}
\end{aligned}
$$

and subsequently $b = -2.6574 * 10^{-4}$ and $a = .3736$ We can also calculate the 0.95 confindence intervals for α and β. $t_{.025}$ equals 2.045 for 31-2= 29 degrees of freedom. For β the confidence interval is calculated as

$$
\begin{aligned}
-2.6574 * 10^{-4} &\pm 2.045\sqrt{\frac{31(1.10294 * 10^{-5})}{1055130}} \\
-2.6574 * 10^{-4} &\pm 3.681 * 10^{-5}
\end{aligned} \tag{D.2}
$$

From this confidence interval for the regression coefficient β we can calculate the line tension. The regression coefficient β corresponds to the slope. The slope for our analysis is $-\sigma/\gamma_{lv}$. For dodecane,

the liquid-vapor surface tension γ_{lv} is $25.44 * 10^{-3} Jm^{-1}$. Multiplying the calculated interval for the slope by γ_{lv} results in

$$\sigma = 6.8 \pm 0.9 \mu Jm^{-1} \tag{D.3}$$

for a 95% confidence interval.

For α the 95% interval is calculated as

$$\begin{aligned} .3736 &\pm 2.045\sqrt{\frac{1.10294 * 10^{-5}(1055130 + (31 \cdot 120.085)^2)}{31 \cdot 1055130}} \\ .3736 &\pm 0.0046 \end{aligned} \tag{D.4}$$

Since the value of a is the y-intercept, which in our case is $\cos\theta_\infty$ we can calculate θ_∞ as $68.1° \pm 0.3°$.

The correlation coefficient is

$$\begin{aligned} r &= \frac{-280.391}{1055130 \cdot 0.084427} \\ r &= -.9394 \end{aligned} \tag{D.5}$$

Appendix E

Grinding and polishing

Diamond embedded drills were secured in a high speed hand drill that was mounted on a lathe as a tool bit would be. The drill could be rotated to an angle relative to the centerline of the lathe and secured in that position. A starter hole through the glass was made using a drill bit approximately 1mm in diameter when the drill bit was parallel to the axis of the glass cylinder. This hole was used as a starting point for the larger bits and those set at angles. Larger conical grinding bits were used at some angle relative to the axis to produce a coarse cone with an internal angle slightly less than the desired angle. Successively finer grits were used to make the walls of the cone smoother and linear over as much of the cone as possible and closer to the final desired angle. The diamond drills would produce a surface that was dimensionally suitable but whose surface was coarse and rough. The tube walls were not transparent at this stage.

The polishing steps would take the tubes from such a coarse stage to a smooth transparent stage where the surface was free from defects. A succession of diamond pastes were used to take the surface from the grinding stage where it was at approximately 200-300 mesh equivalent to the final point which had a mesh equivalent of 100,000. Cylindrical toothpicks were used as phenolic tools. They were rolled in a small amount of diamond paste with enough force to impress the diamond compound into the surface. A paste of 325 was first used. The phenolic tool was inserted in the high speed drill while the glass tube was rotated in an opposite direction using either a lathe or an improvised rotating fixture. The 325 grit is a rough grit

which was used to remove larger imperfections in the tube that were introduced during the drilling and grinding operations.

An extender fluid was used to lubricate the surface and enhance the polishing action of the compounds. Several phenolic tools were expended at each level of polishing. When the 325 mesh equivalent produced no more noticeable changes as observed under a microscope, the next paste of 600 was used, followed by 1200, 3000, 14000 and finally 100000. If defects were apparent at any level that were larger than those that should have been removed previously, then the process was started again using a sufficiently coarse grit. Contamination could occur if any of the larger grit became mixed in with the finer pastes. It was also important that the phenolic tools used did not become contaminated at any point of the polishing steps. It was essential at every step that the tube itself was cleaned of the diamond compound before the next abrasive was used. Any compound left in the glass tube or contaminating the phenolic tool would leave surface scratches that had to be removed by redoing the entire conical tube.

Bibliography

[1] D. Li,Colloids and Surfaces,116(1996)1-23

[2] F.Y.H. Lin, D. Li Colloids Surfaces A: Physicochemical and Engineering Aspects 87 (1994) 93-100

[3] J.W. Gibbs, The Scientific Papers, Vol 1, Dover, New York, 1961, p.288

[4] J.W. Gibbs, Collected Works of J.W. Gibbs, Vol 1, Yale Univ. Pr., New Haven, Conn. (1928)

[5] A.I. Rusanov, The Centennial of Gibbs' Theory of Capillarity, in: The Modern Theory of Capillarity., (F.C. Goodrich and A.I. Rusanov,eds.), pp. 1-18, Akademie-Verlag, East Berlin (1981)

[6] R.J. Good and M.N.Koo,J. Colloid Interface Sci.,71(1979)283.

[7] J.Gaydosand A.W. Neumann,J. Colloid Interface Sci.,120(1987)76.

[8] D. Li and A.W. Neumann,J. Colloid Interface Sci., 43(1990)195.

[9] D. Duncan,D.Li,J. Gaydos and A.W. Neumann,J. Colloid Interface Sci.,169(1995) 256

[10] T.Young, Philos, Trans. R. Soc. London, 95 (1805) 65.

[11] A.W. Neumann and R.J. Good,J. Colloid Interface Sci.,38 (1972) 341

[12] R.N. Wenzel, Ind. Eng. Chem.,28 (1936) 988

[13] A.B.D. Cassie and S. Baxter, Trans. Faraday Soc., 40 (1944) 546

[14] R. Shuttleworth and G.L. Bailey, Discuss. Faraday Soc., 3 (1948)16

[15] B.V. Derjaguin C.R. Acad. Sci. USSR, 51 (1946) 361

[16] A.B. Ponter and A.P. Boyes, Can. J. Chem.,50(1972) 2419

[17] A.B. Ponter and A.P. Boyes,J. Chem. Eng. Jpn. 7 (1974)314

[18] A.B. Ponter and M. Yekta-Fard,Colloid Polym. Sci.,263(1985)1

[19] M. Yekta-Fard and A.B. Ponter, J. Colloid Interface Sci., 126(1988) 134

[20] J. Drelich and J. Miller, Colloids Surf., 69 (1992) 35

[21] J. Drelich,J. Miller, and J. Hupka, J. Colloid Interface Sci.,155(1993)385

[22] Drelich and J. Miller, J. Colloid Interface Sci.,164 (1994)252

[23] J.Langmuir,J. Chem. Phys.,1(1993)756

[24] D.Li and D.J. Steigmann, Colloids Surf., 106(1996) ???

[25] D.J. Steigmann and D.Li,IMA J. Appl. Math., 55 (1995) 5464

[26] H.B. Callen, Thermodynamics and an Introduction to Thermostatistics,Wiley,New York, 2nd ed., 1985

[27] J.W. Gibbs, The Scientific Papers Vol. 1 Dover New York, 1961 p.296

[28] W.D. Harkins, J.Chem. Phys., 5 (1937) 135.

[29] F.P. Buff and H.J. Saltsburg, Chem. Phys., 26 (1957)23.

[30] J.S. Rowlinson and B. Widom, Molecular Theory of Capillarity, Oxford Science Publications, New York, 1984

[31] K. Nishikawa and T. Ito, Heat Transfer in Energy Problems, in T. Mienshina and W.J. Yang(Eds.), Proc. of a Seminar Sponsored by the United States-Japan Cooperative Science Program, September 23-Octorber 2,1980, Tokyo, Japan, Hemisphere Publishing Corporation, Washington, 1983

[32] S. Yamali and H. Merte, Jr., in C.T. Avedisian and T.M. Rudy (Eds.), Fundamentals of Phase Change: Boiling and Condensation, American Society of Mechanical Engineers, New York, 1984,p.143.

[33] A.W.Neumann and R.J. Good, in R.J. Good and R.R. Stromberg (Eds.), Surfaces and Colloid Science, Vol.11, Plenum,New York,1979,p.31

[34] Y. Gu D. Li and P. Cheng,J. Colloid Interface Sci., Vol 180 (1996)212-217

[35] D. Li P. Cheng and A.W. Neumann, Adv. Colloid Interface Sci.,39(1992) 347.

[36] Y. Rotenberg L.Boruvka and A.W. Neumann,J. Colloid Interface Sci.,93(1983)169

[37] P.Cheng, Ph.D. Thesis University of Toronto Canada,1990.

[38] L.Boruvka and A.W. Neumann, J. Chem Phys.,66(1977)5464

[39] George A. Ferguson and Yoshio Takane,Statistical Analysis in Psycholog and Education,6th edn. McGraw-Hill New York 1989